# Auroral processes in satellite data


*Tomas Karlsson*

*Space and Plasma Physics, School of Electrical Engineering*

*Royal Institute of Technology, Stockholm*

*Sweden*

# Overview

- Setting the scene
- Auroral processes in the upward current region
- Auroral processes in the downward current region
- Dayside and cusp aurora, theta aurora
- Temporal evolution in the auroral zone

## *Very useful reference:*

# *Space Science Series of ISSI*
# Auroral Plasma Physics

*Götz Paschmann, Stein Haaland, Rudolf Treumann*

(Space Science Reviews, vol 103, 1-4, 2002)

# Auroral ovals

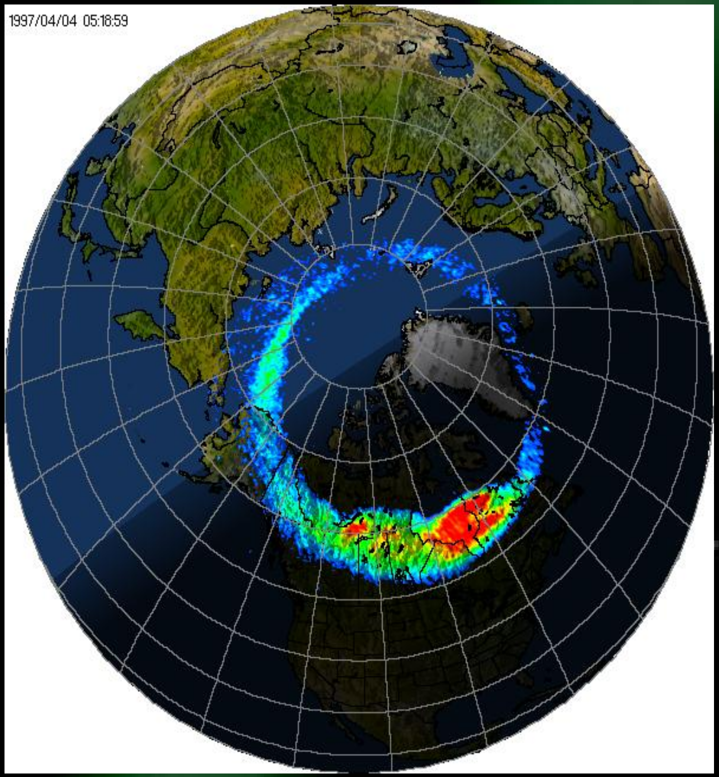


Polar

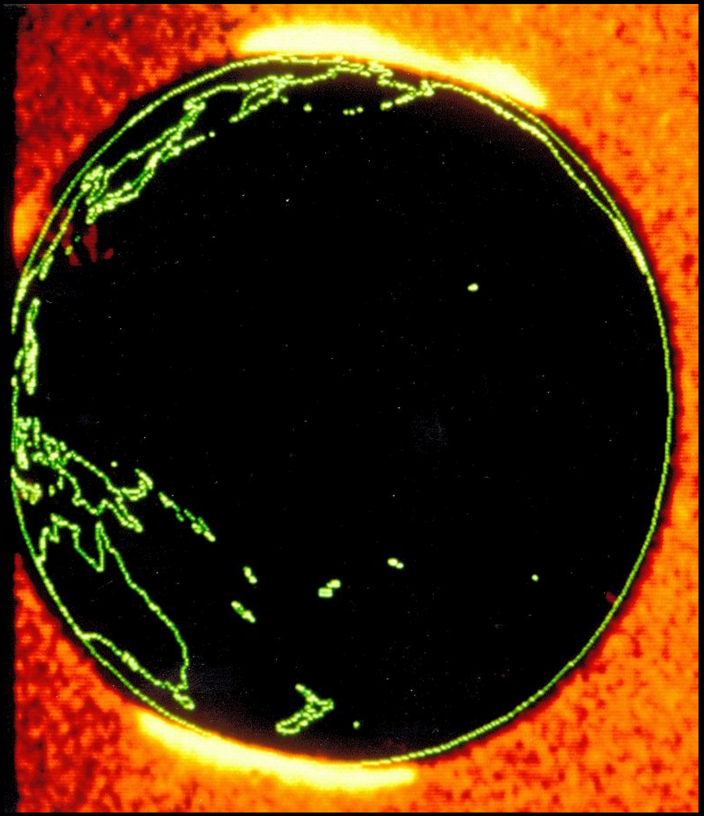

Dynamics Explorer

# The auroral oval is the projection of the plasmasheet onto the atmosphere

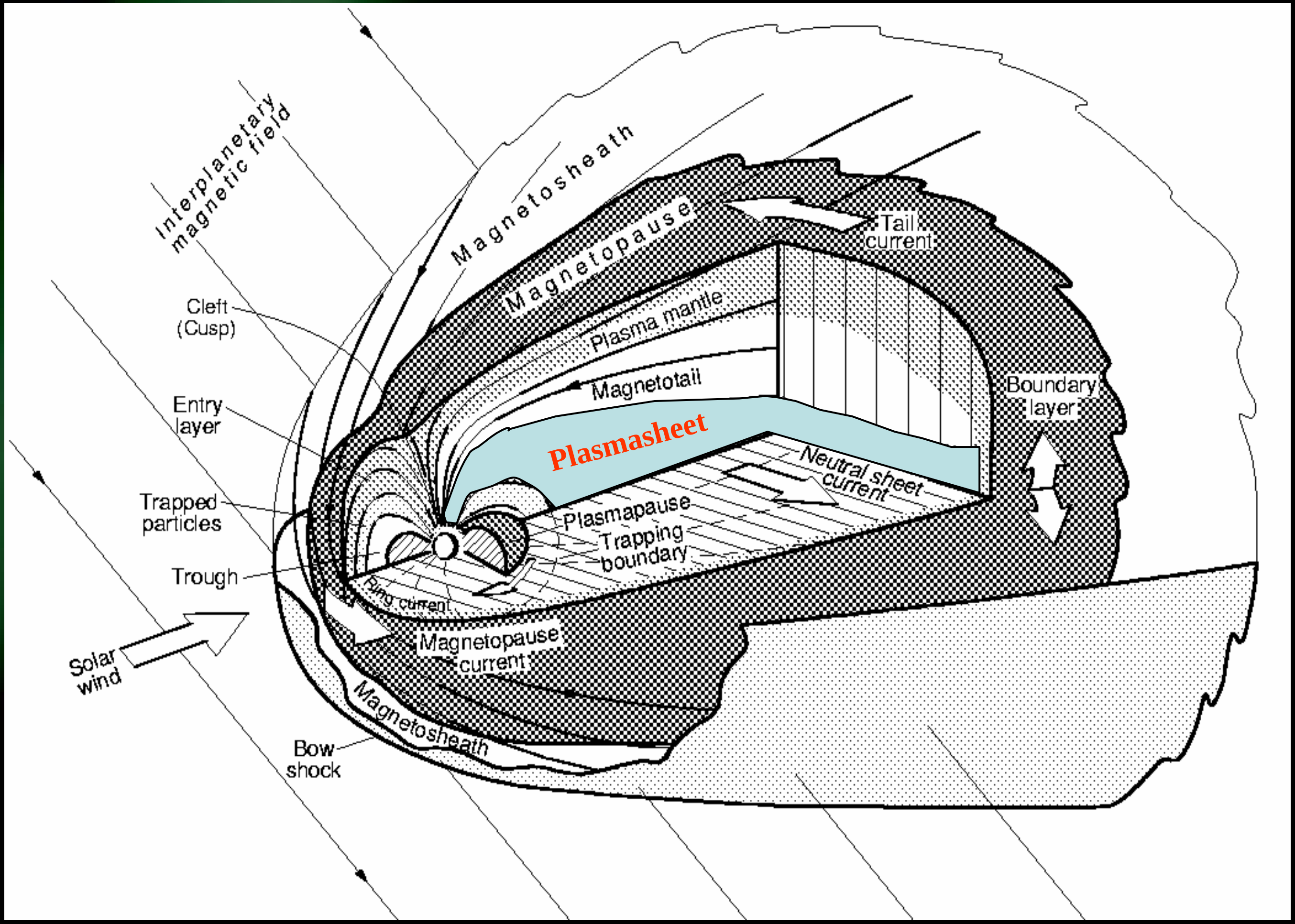

# Auroral emissions

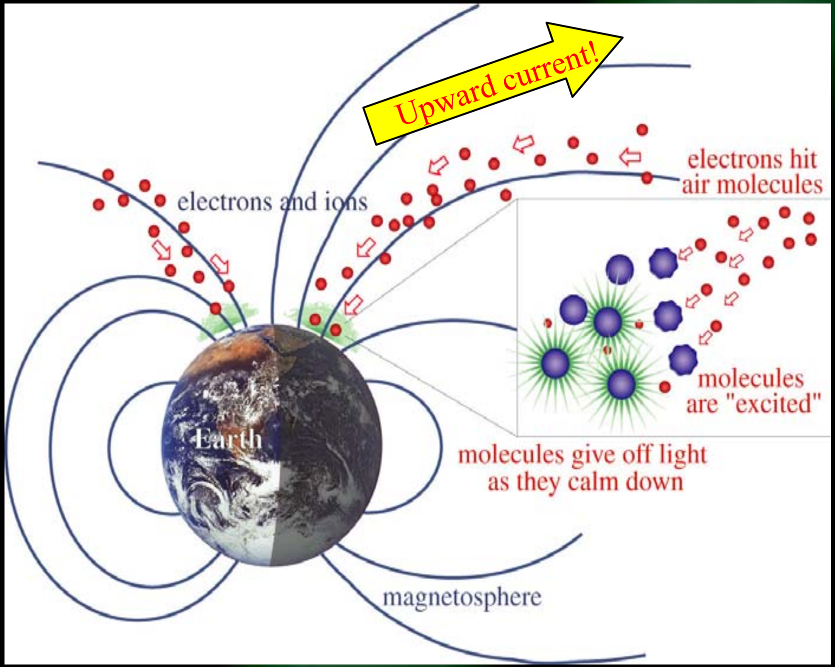


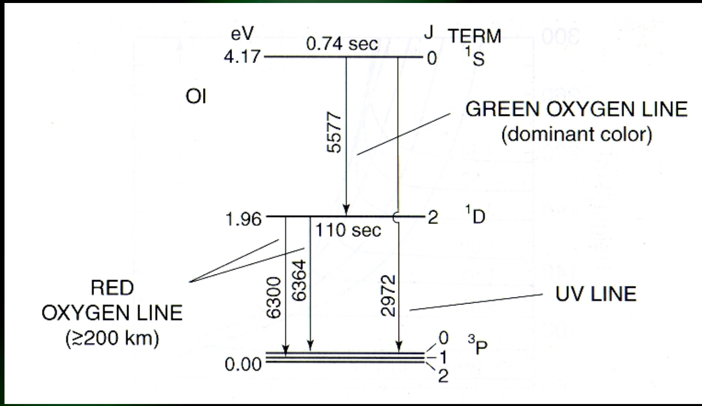


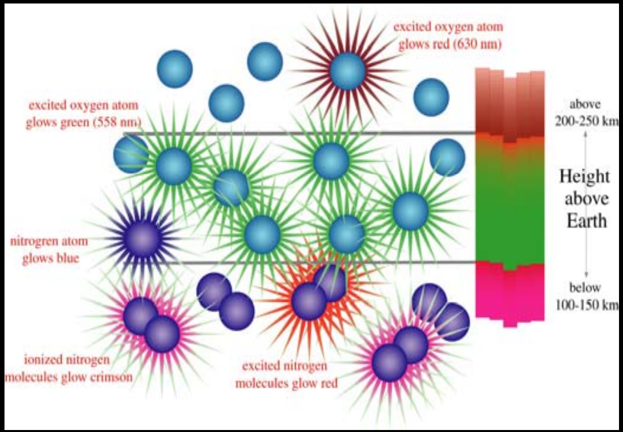

# Homogenous auroral arcs

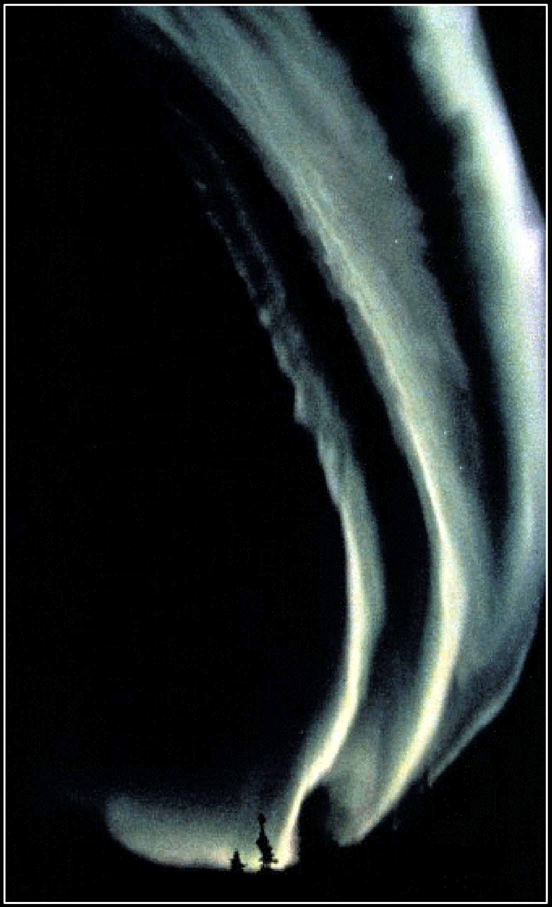

# Particle motion in the geomagnetic field

**gyration** **longitudinal oscillation** **azimuthal drift**

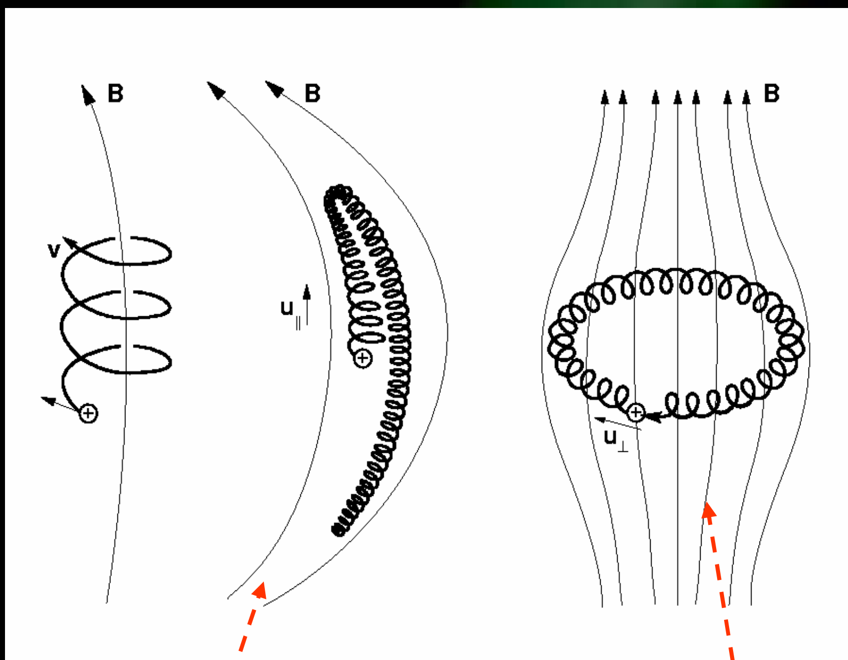


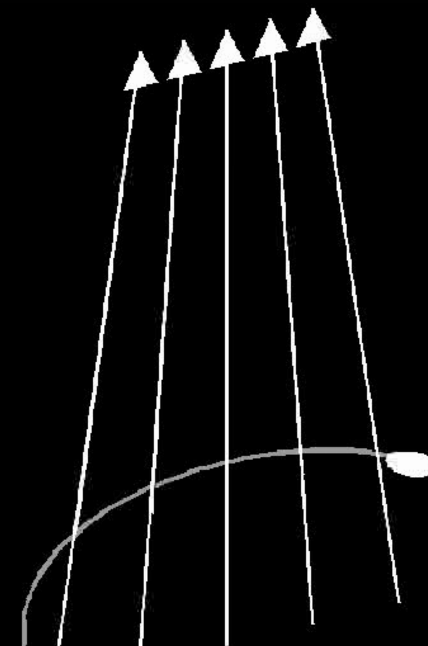

Magnetic mirror

grad B drift

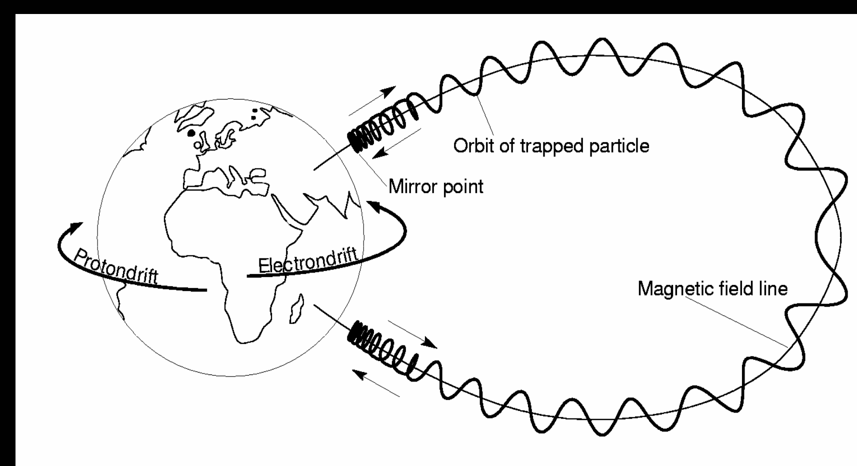

# Magnetic mirror

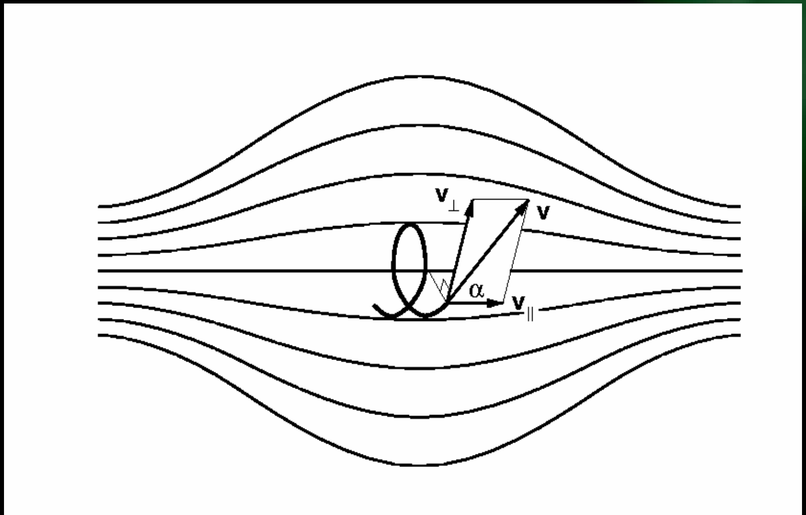


mv²/2 constant →

$$\frac{\sin^2\alpha}{B} = const$$

particle turns when α = 90° →

$$B_{turn} = B/\sin^2\alpha$$

If maximal B-field is $B_{max}$ a particle with pitch angle $\alpha$ can only be turned around if

$$B_{turn} = B/\sin^2\alpha \le B_{max}$$ →

$$\alpha > \alpha_{lc} = \arcsin\sqrt{B/B_{max}}$$

The magnetic moment $\mu$ is an ***adiabatic invariant***.

$$\mu = \frac{mv_\perp^2}{2B} = \frac{mv^2\sin^2\alpha}{2B}$$

Particles in ***loss cone*** : $\alpha < \alpha_{lc}$

# Magnetospheric convection

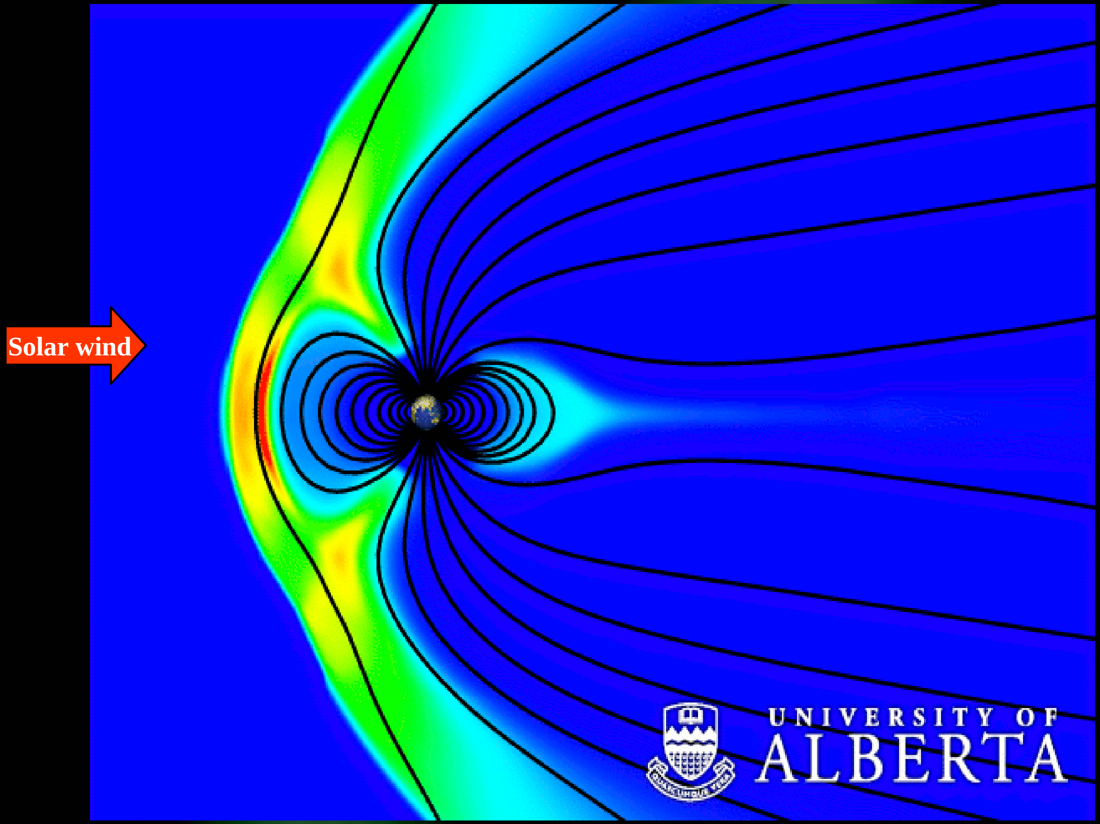


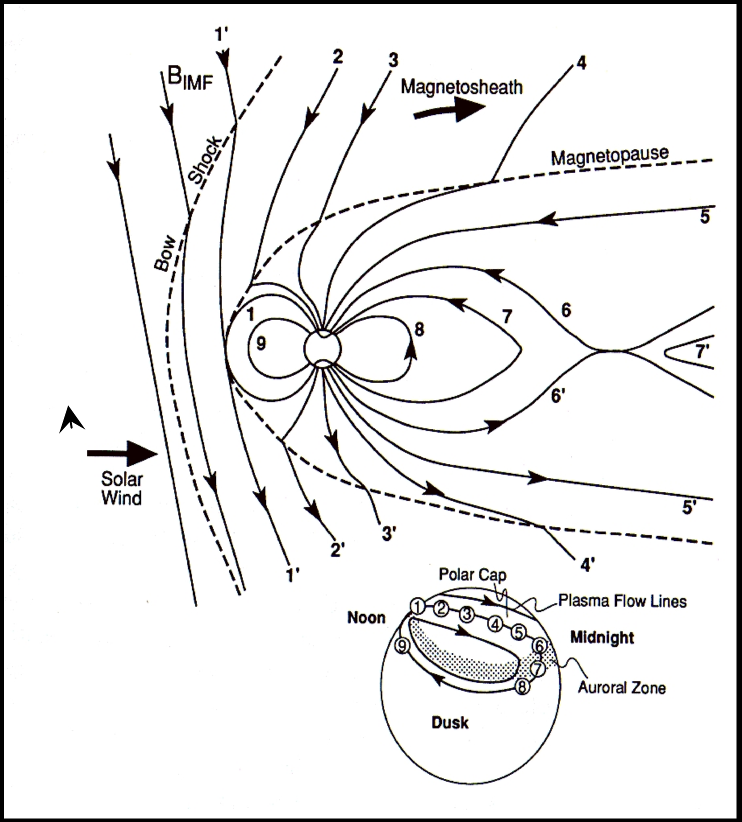

# Atmospheric collisions - emissions

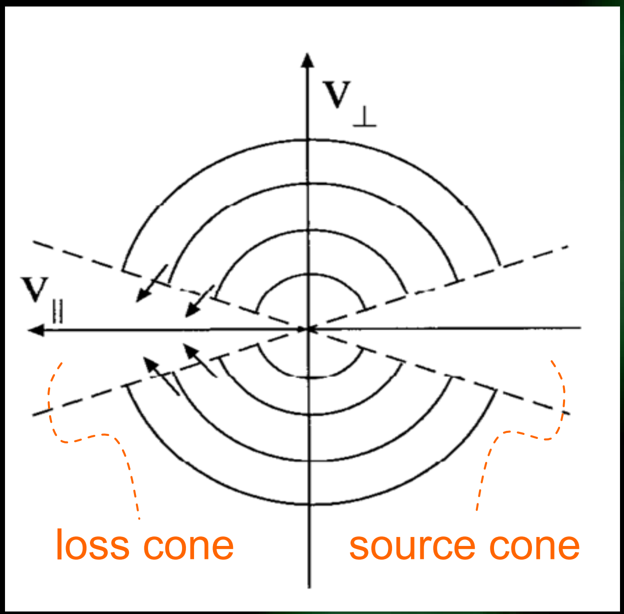


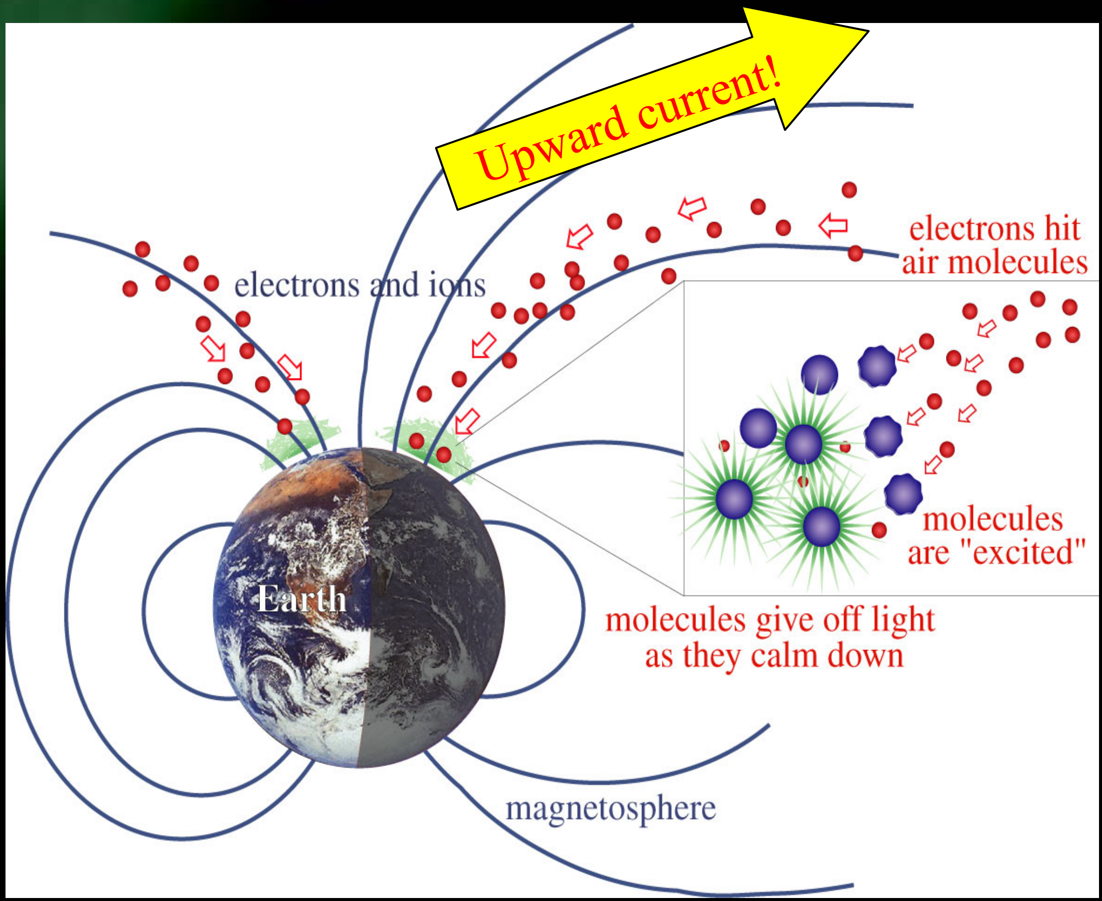

# A typical auroral pass - CLUSTER

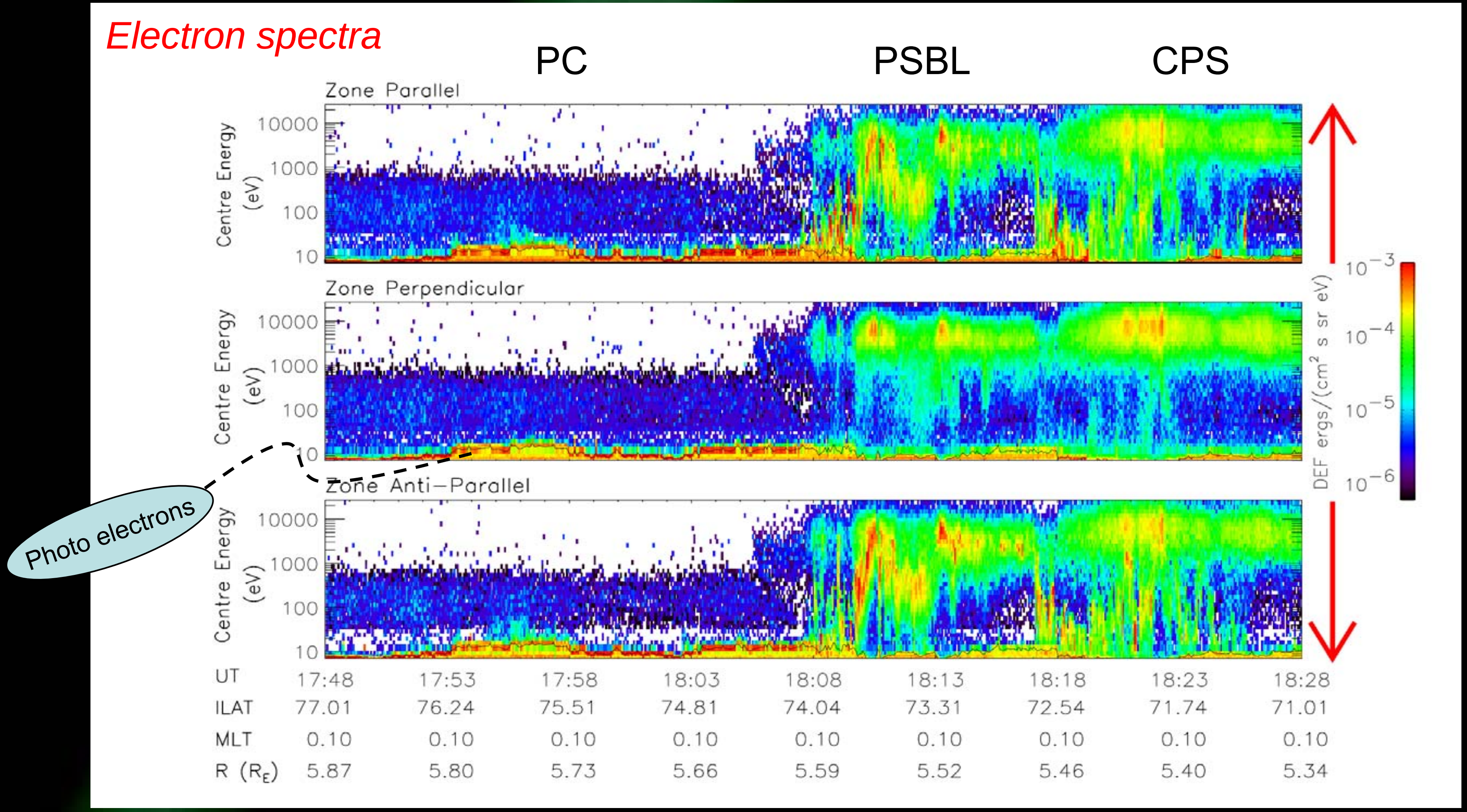

# Auroral scales

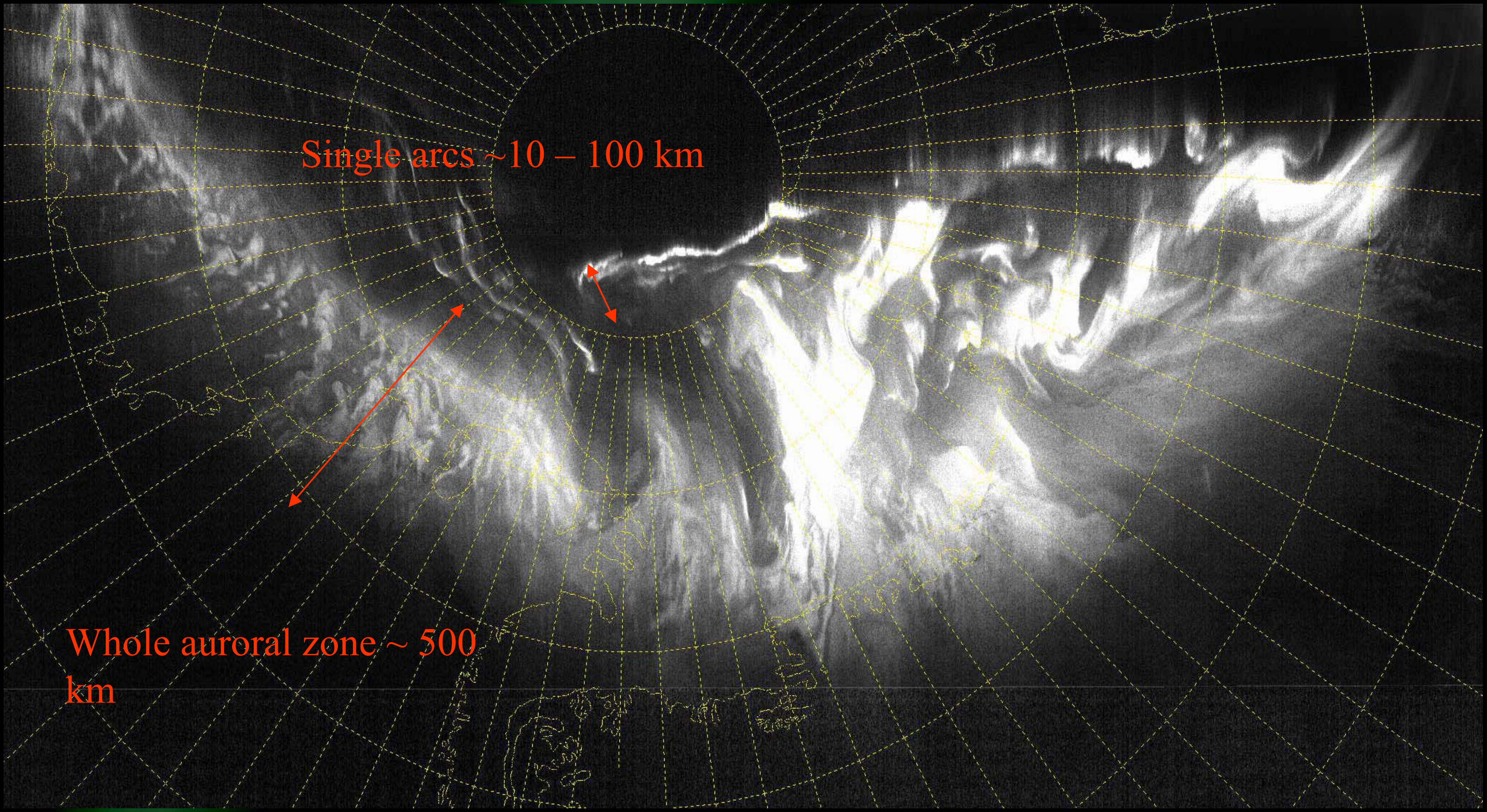


*Photo from DMSP satellite*

# Birkeland currents in the auroral oval

Low geomagnetic activity High geomagnetic activity

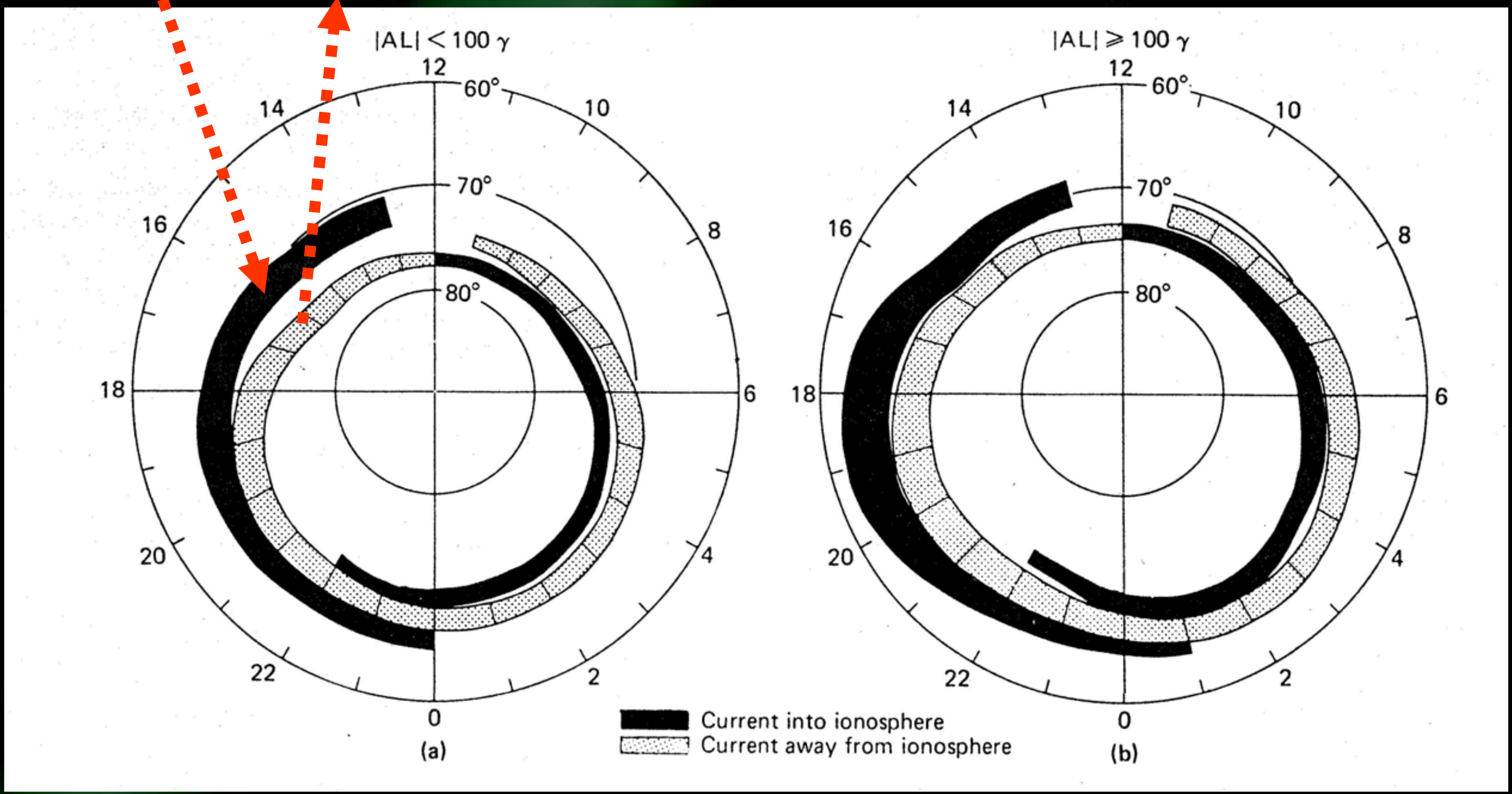

# A typical auroral pass - FAST

$\Delta B_{EW}$

dE-flux, $e^-$

PA, $e^-$

dE-flux, $e^-$

n-flux, $e^-$

E-flux, $e^-$

dE-flux, $i^+$

PA, $i^+$

E-perp (DC)

E (AC)

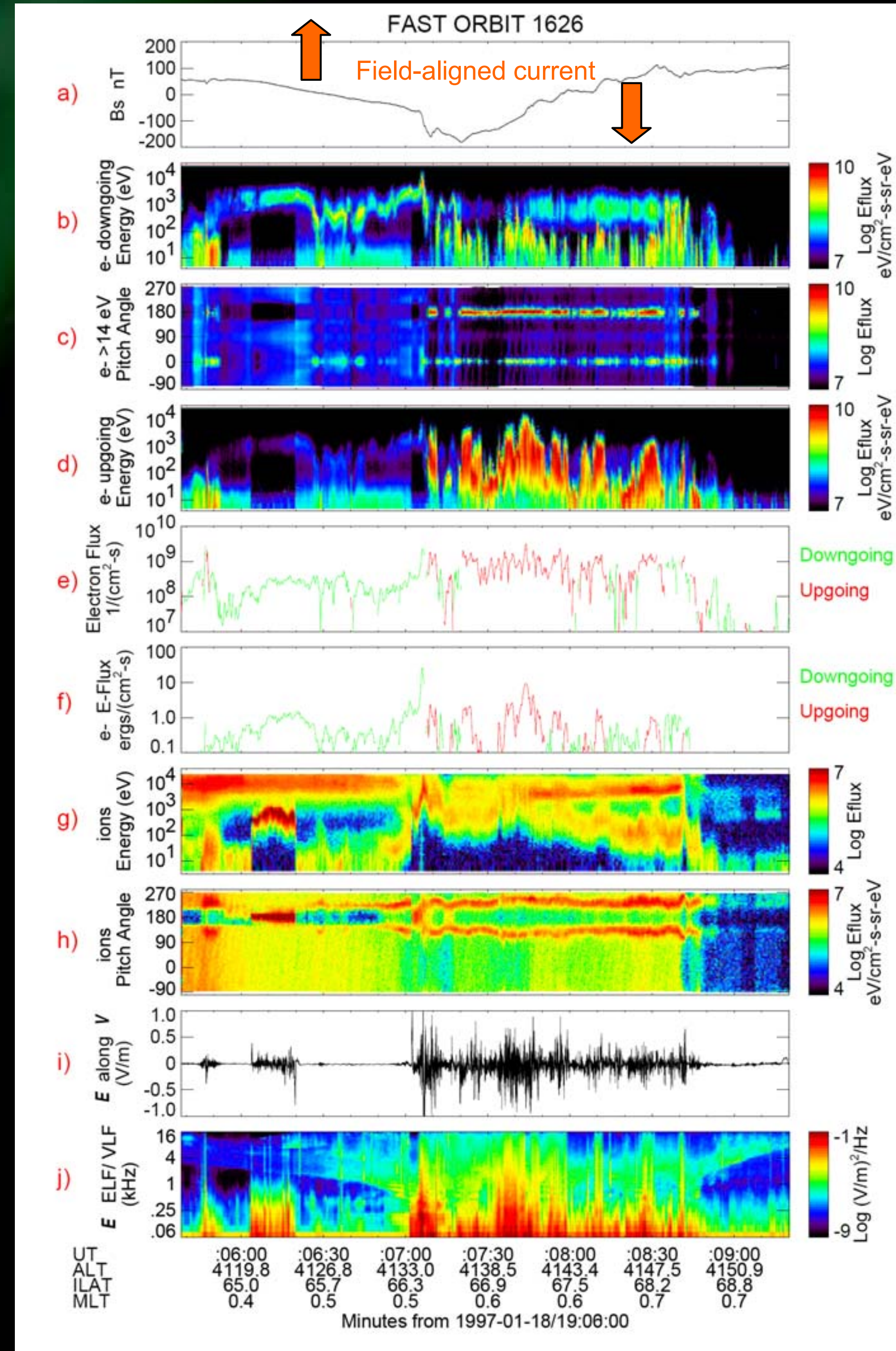


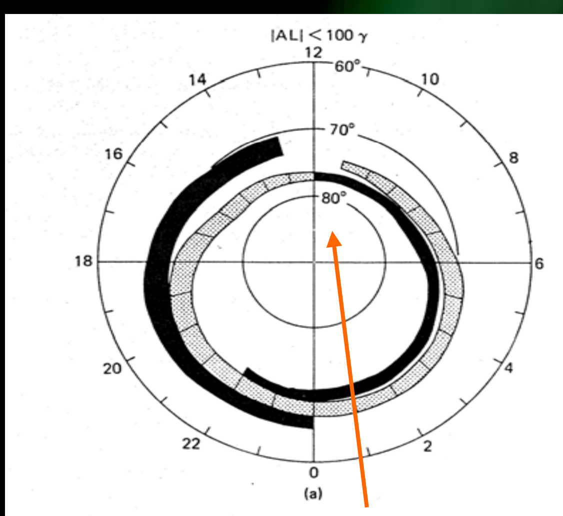

# Current sheet approximation and Ampére's law

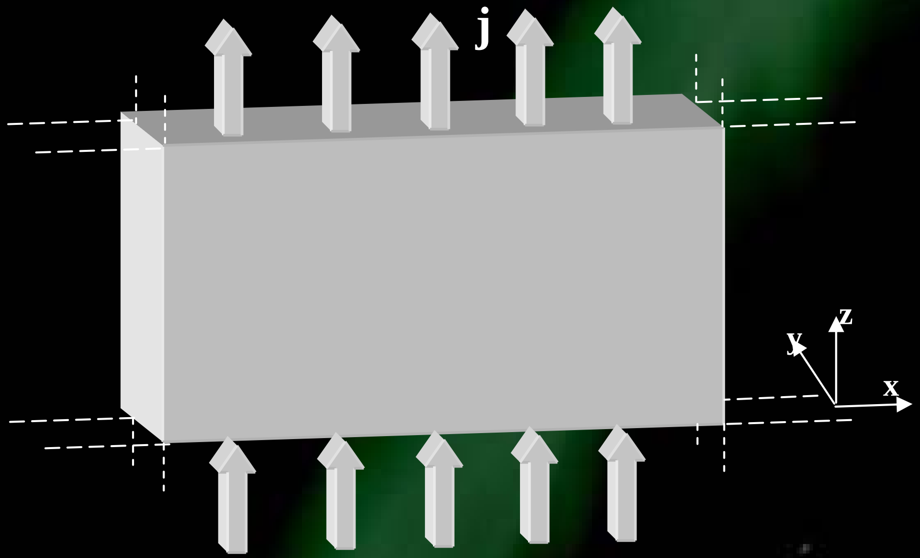


$$\left(\frac{\partial B_z}{\partial y}-\frac{\partial B_y}{\partial z},\ \frac{\partial B_x}{\partial z}-\frac{\partial B_z}{\partial x},\ \frac{\partial B_y}{\partial x}-\frac{\partial B_x}{\partial y}\right)=\mu_0\left(j_x,\ j_y,\ j_z\right)$$

But $\frac{\partial}{\partial x} = 0$ and $\frac{\partial}{\partial z} = 0$

$$\left(\frac{\partial B_z}{\partial y},\ 0,\ -\frac{\partial B_x}{\partial y}\right)=\mu_0\left(0,\ 0,\ j_z\right)$$

**Ampére's law (no time dependence):**

$$\nabla\times\mathbf{B}=\mu_0\mathbf{j}$$

$$j_z=-\frac{1}{\mu_0}\frac{\partial B_x}{\partial y}$$

# Current sheet

## Determination of current density by magnetic field measurement

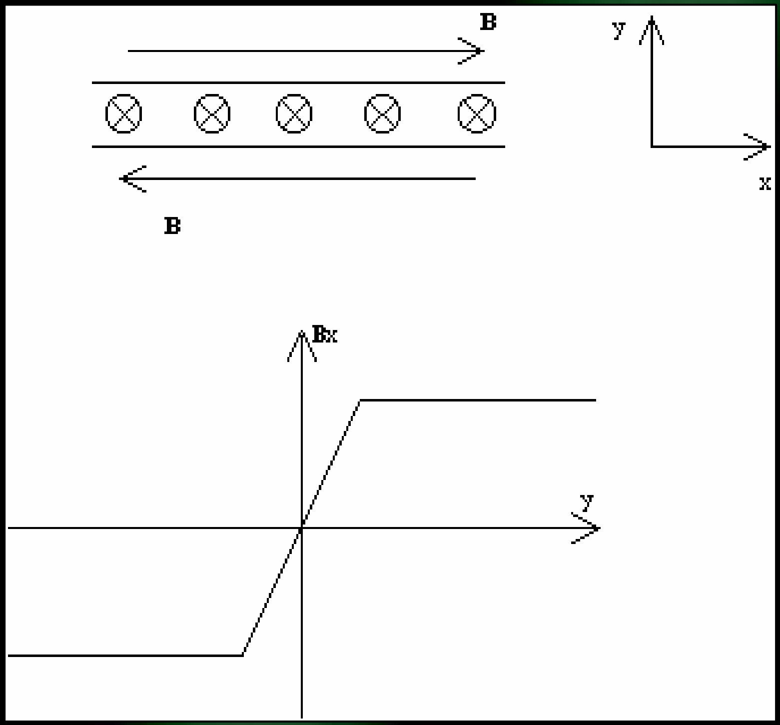


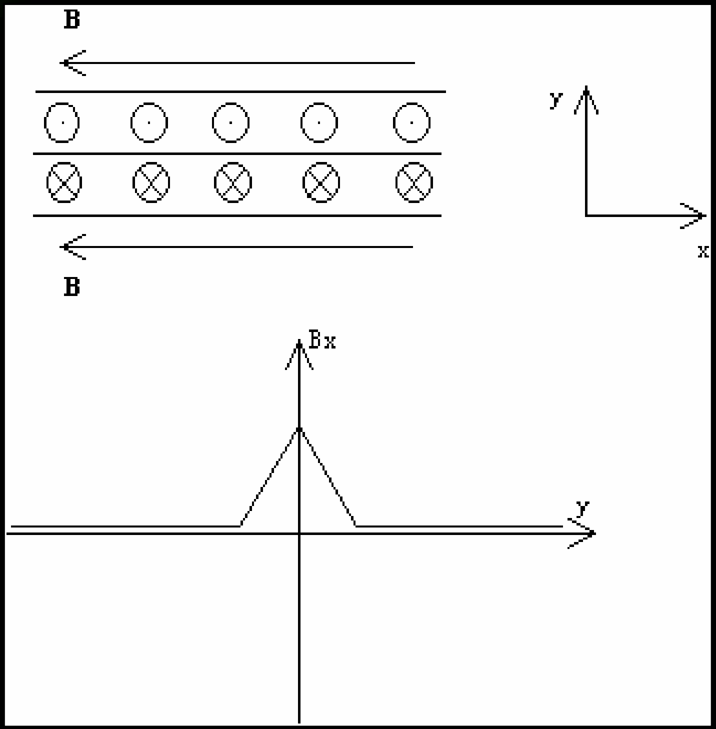


$$j_z = -\frac{1}{\mu_0}\frac{\partial B_x}{\partial y}$$

# Upward and downward current regions

Inverted V

Upgoing electron beams

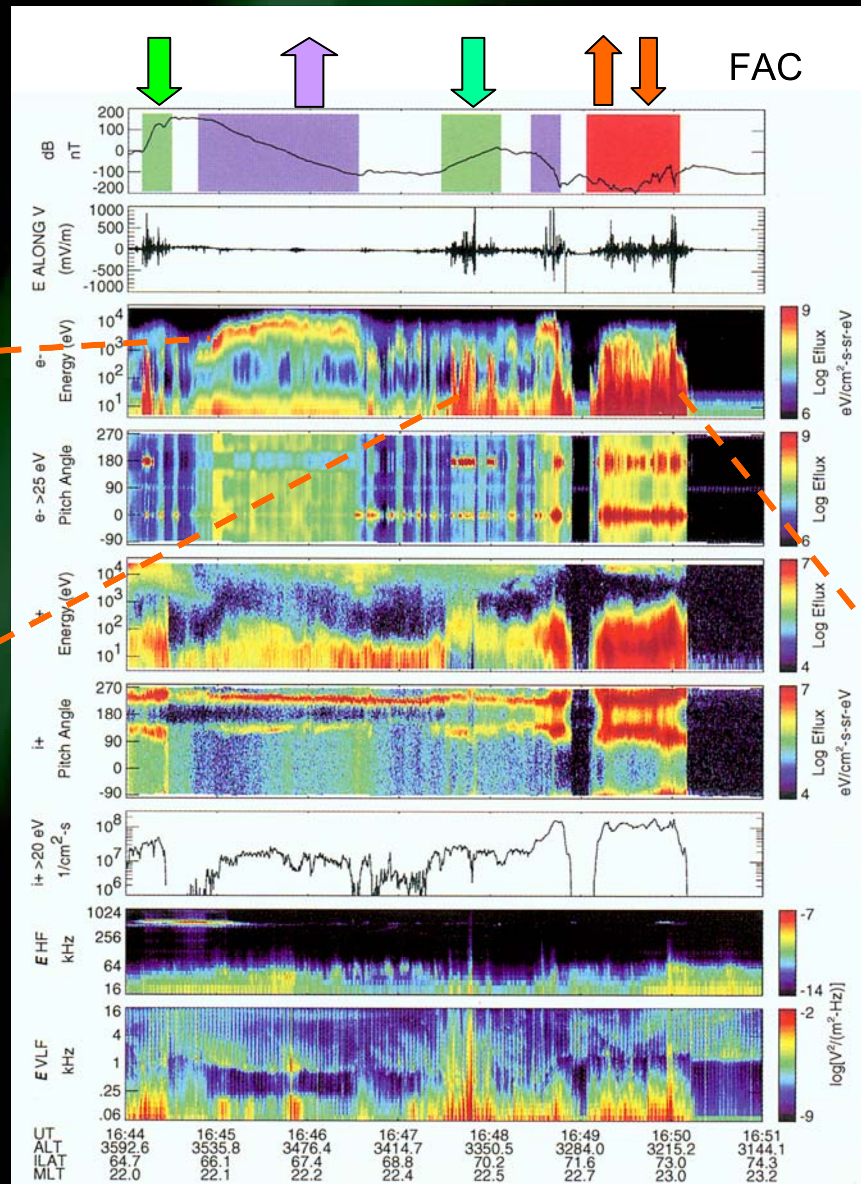


180° =

0° =

Alfvénic aurora

# Upward current region

## Inverted V arc

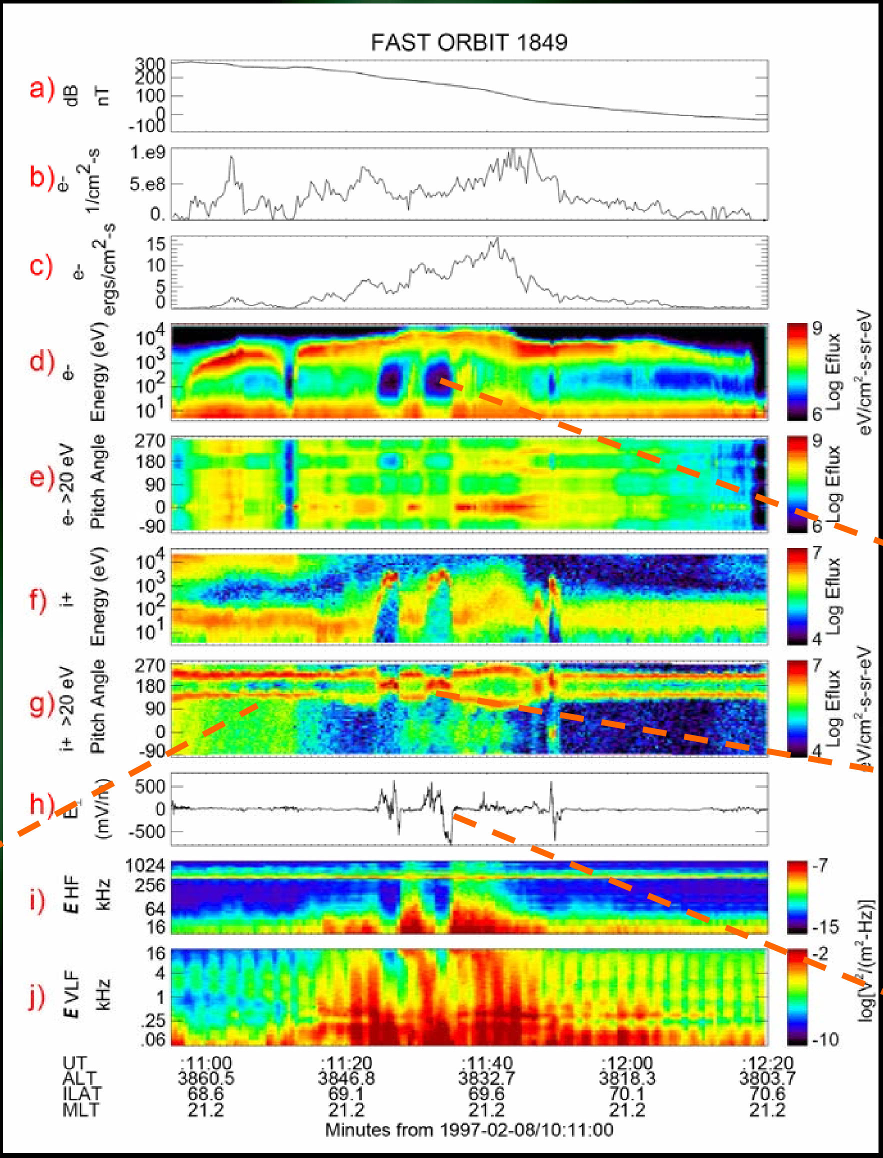


Visual limit ~ $10^{-3}$ $Jm^{-2}s^{-1}$ =1 erg $cm^{-2}s^{-1}$

180° = ⬆

0° = ⬇

# Satellite signatures of U potential

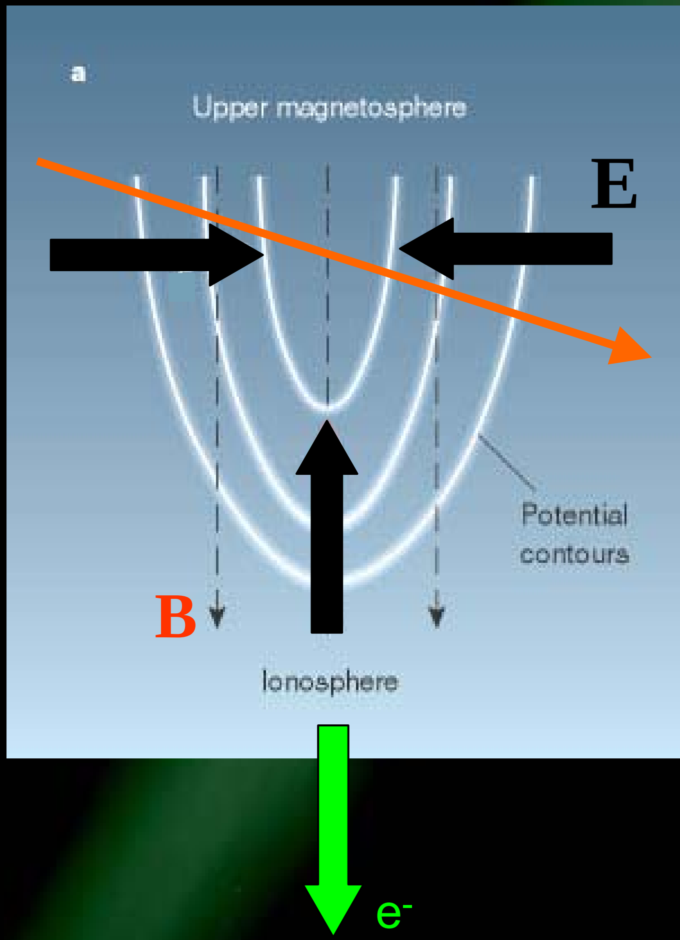


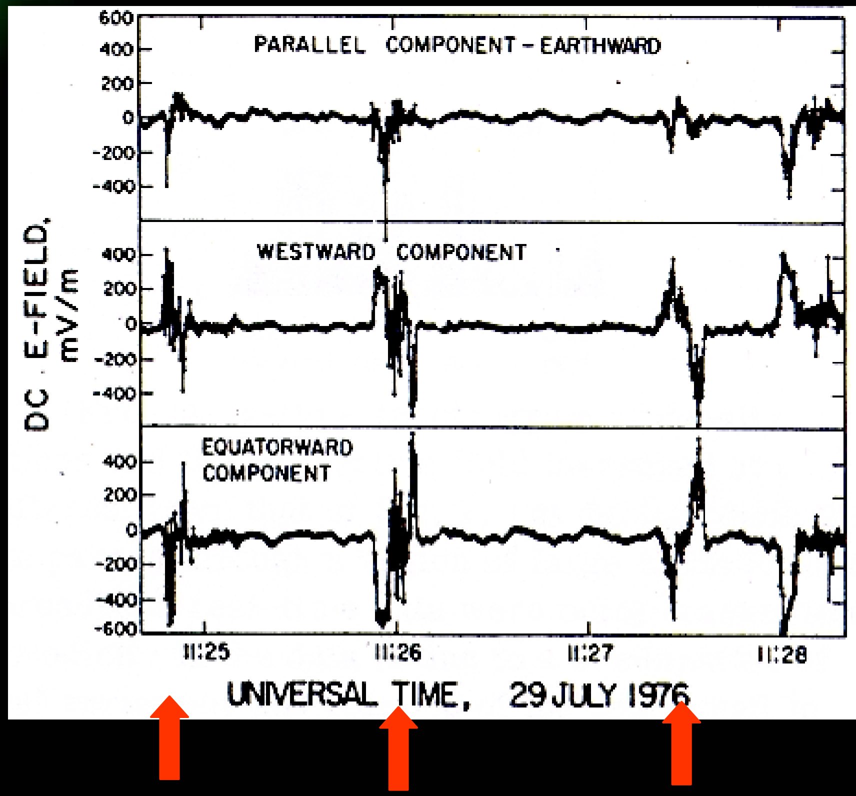


Measurements made by the ISEE satellite (Mozer et al., 1977)

# Acceleration potential structure I

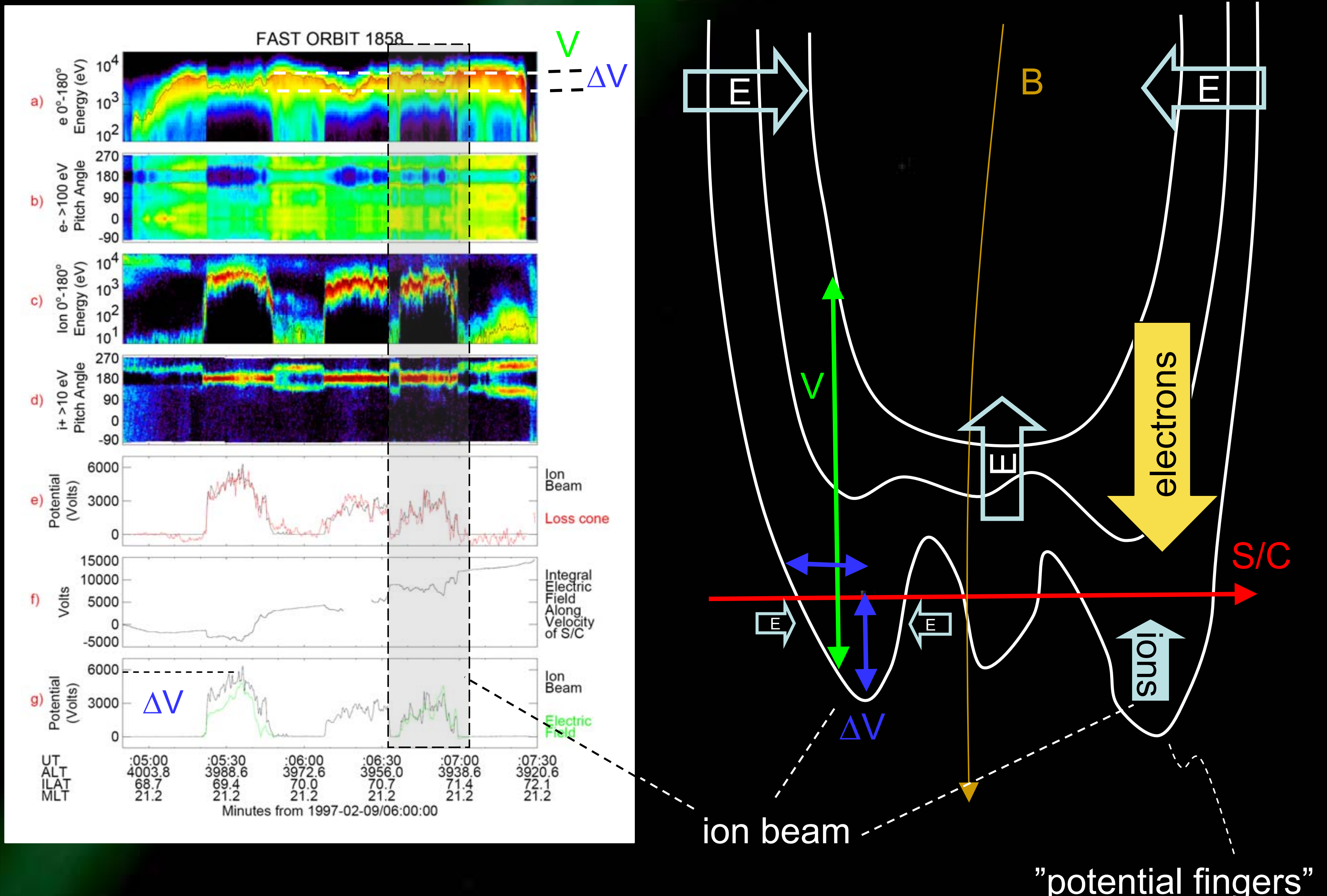

# Acceleration potential structure II

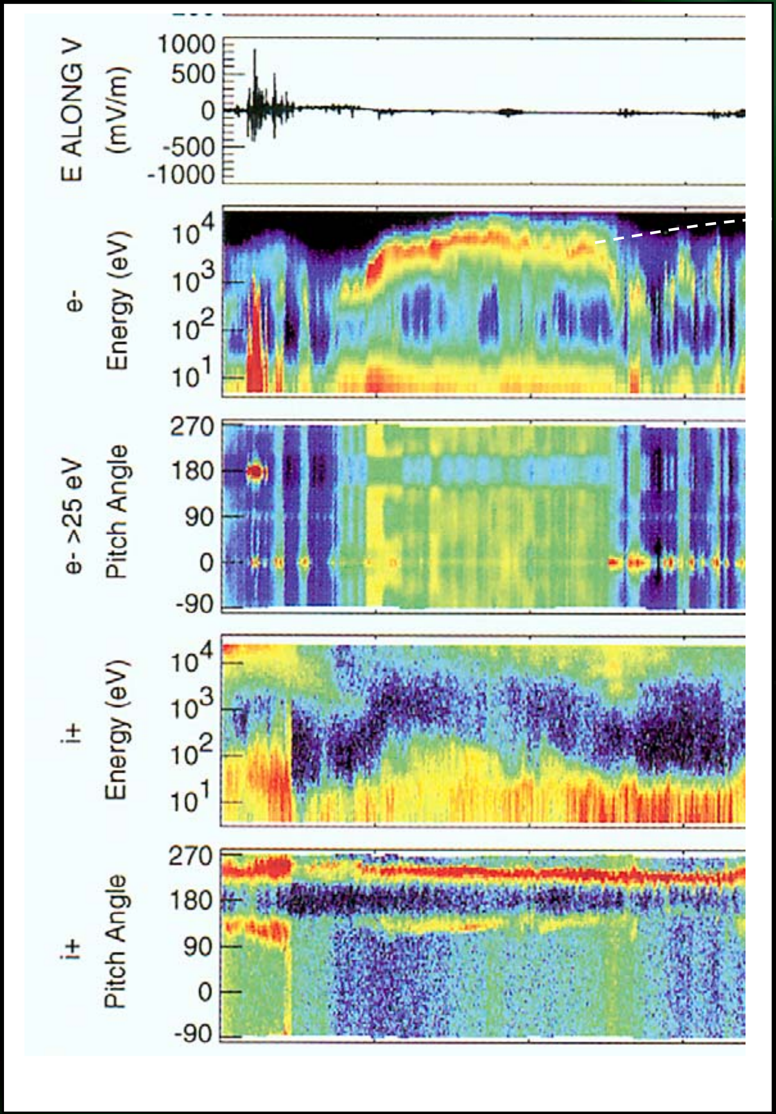


Localized regions of higher energy electrons without associated ion beams

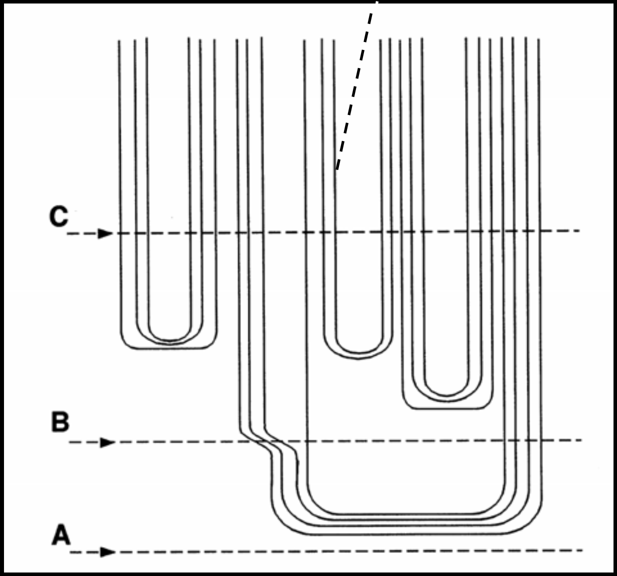

# Why particle acceleration?

- The magnetosphere often acts as a current generator
- Electrons are accelerated downwards by upward E-field.
- This increases the pitch-angle of the electrons, and more electrons can reach the ionosphere, where the current can be closed.

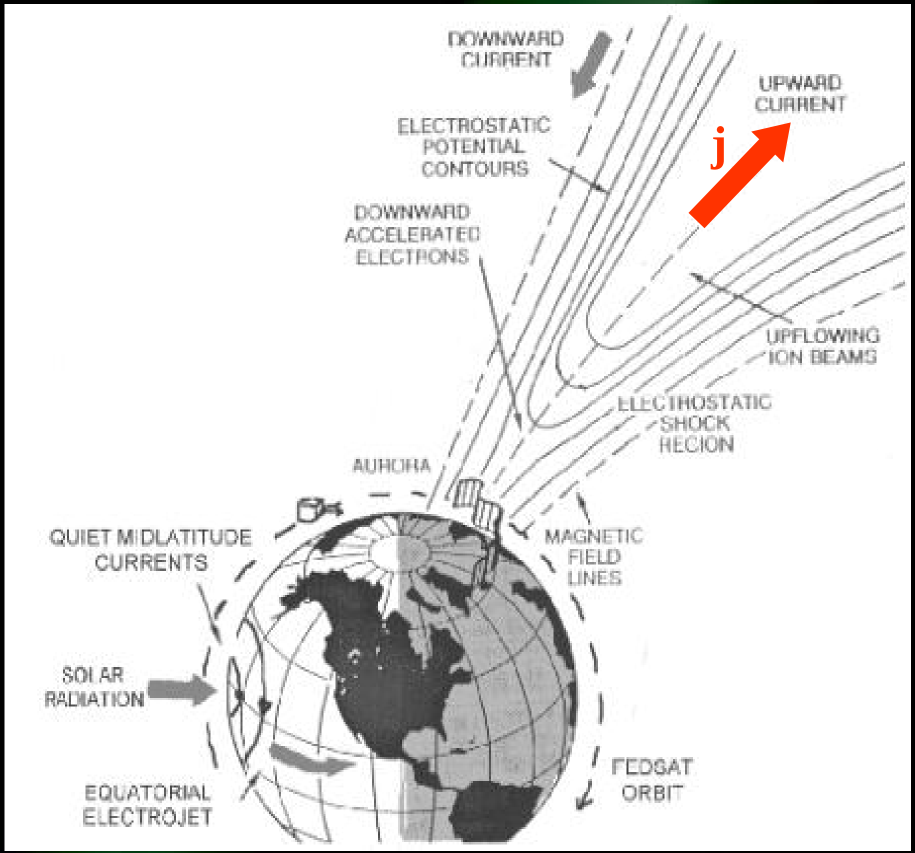


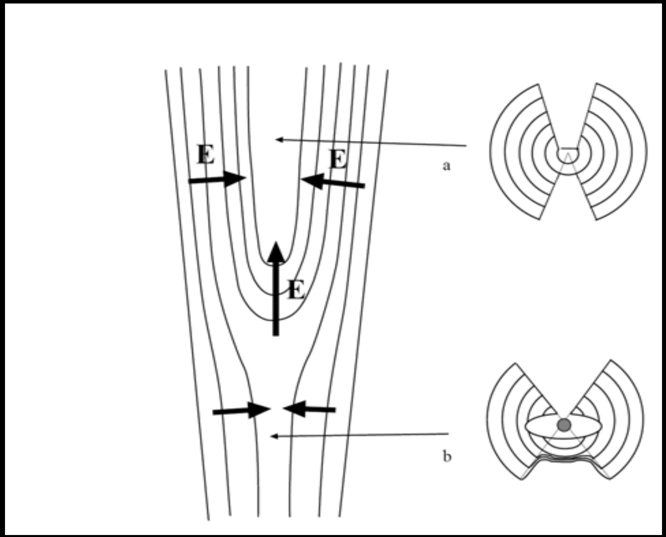

# Auroral currents – Knight relation

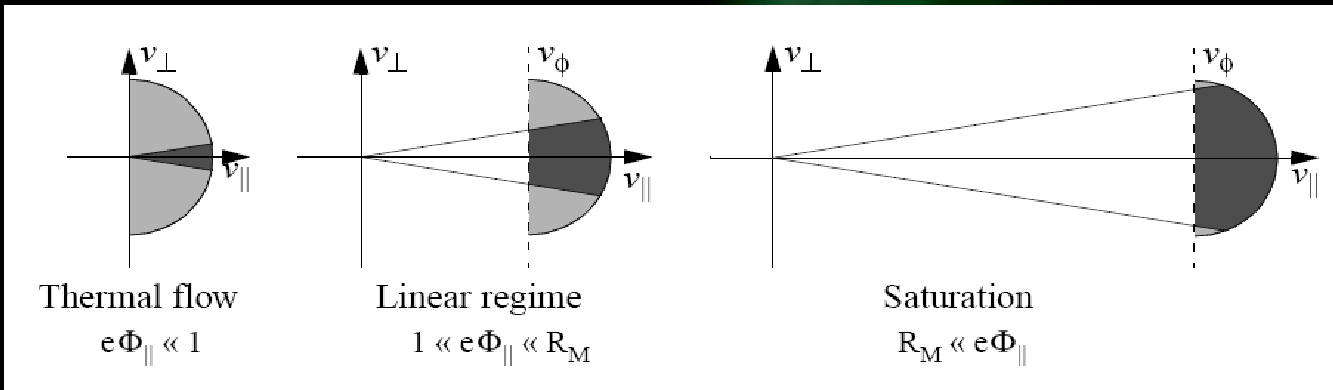


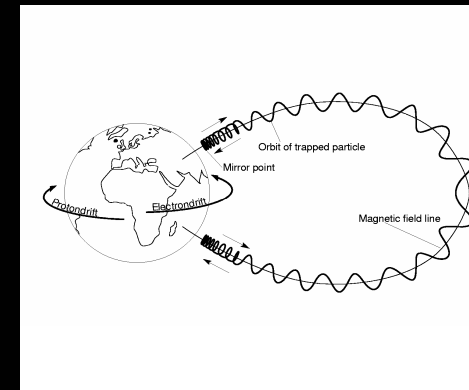


Fraction of particles in the loss cone:

$$f = \frac{\pi\theta_{lc}}{2\pi} \sim \frac{B_{ms}}{B_{ion}} \sim 2\times10^{-4}$$

Thermal current:

$$j_{||,ms} = n_0 e v_{th} f$$

$$j_{||,ion} = n_0 e v_{th} f \frac{B_{ms}}{B_{ion}} =$$

$$= n_0 e v_{th} \frac{B_{ms}}{B_{ion}} \frac{B_{ion}}{B_{ms}} = n_0 e v_{th} \approx$$

$$\left[n_e = 0.1\,\mathrm{cm}^{-3}, T_e = 1\,\mathrm{keV}\right] \approx$$

$$\sim 1\,\mu\mathrm{A/m}^2$$

Apply a parallel potential drop:

$$j_{||,ion} = n_0 e v_{th} \frac{B_{ion}}{B_{ms}} \left[1 - \frac{e^{-xe\Phi_{||}/T_e}}{1+x}\right]$$

Linear regime :

$$j_{//,ion} \approx n_0 e v_{th} \frac{e\Phi_{//}}{k_B T_e} = K\Phi_{//}$$

$$K = \frac{e^2 n_0}{\sqrt{2\pi m_e k_B T_e}} \sim 10^{-9}\ \mathrm{S/m}^2$$

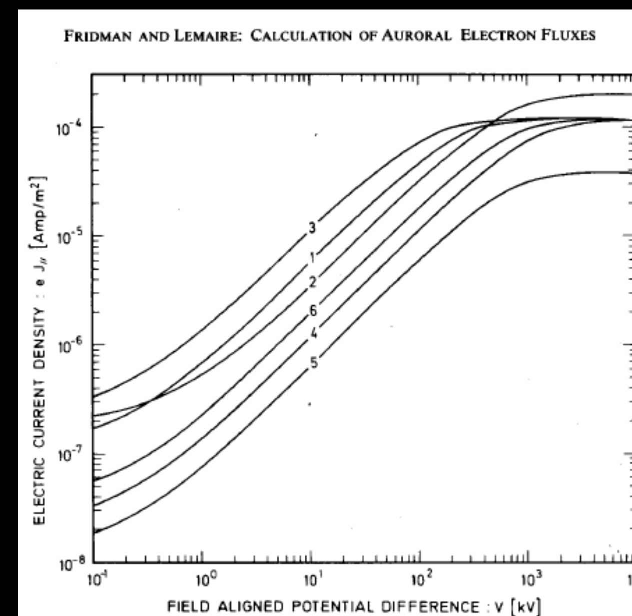


$$v_{th} = \sqrt{T_e / 2\pi m_e} \qquad x = \frac{1}{B_I / B_0 - 1}$$

# Particle distributions associated with inverted V's

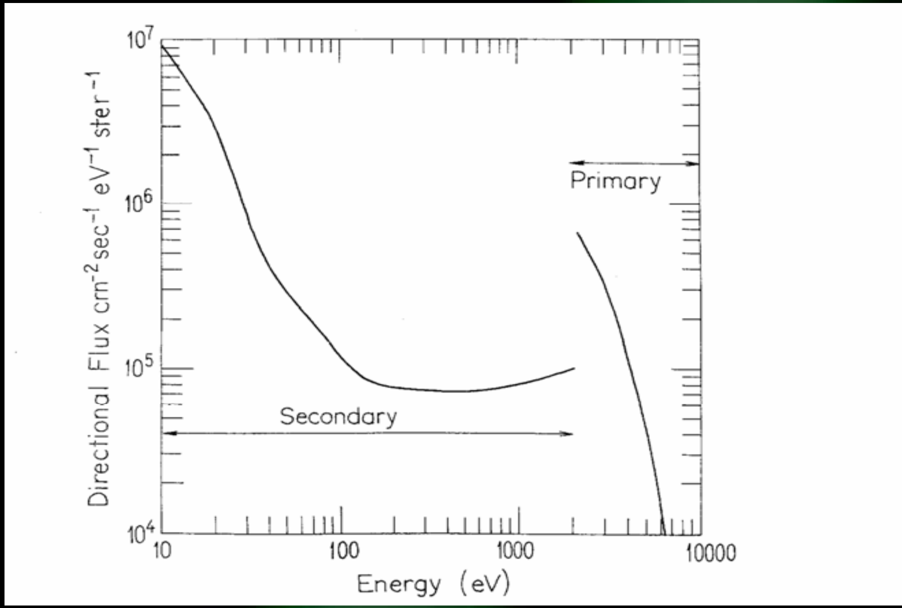


Model of cold beam producing secondaries (Evans, 1974)

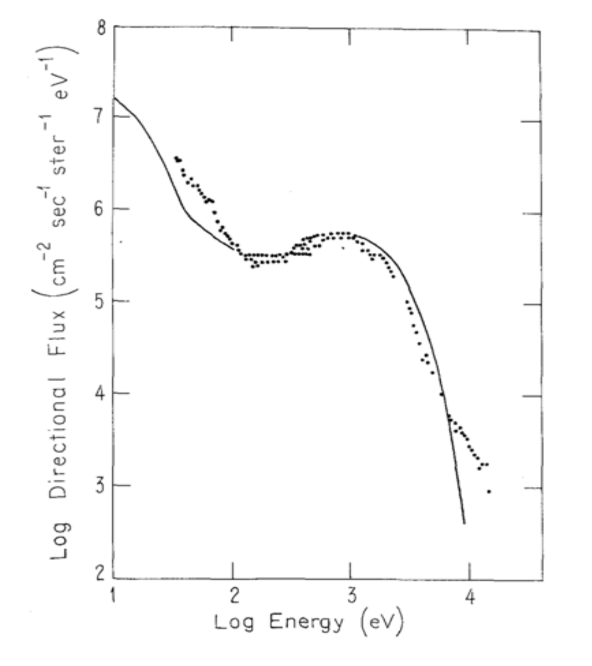


Model of hot electron beam and second<aries (Evans, 1974). Data from Franck and Ackerson, 1971

# Auroral cavity and trapped populations

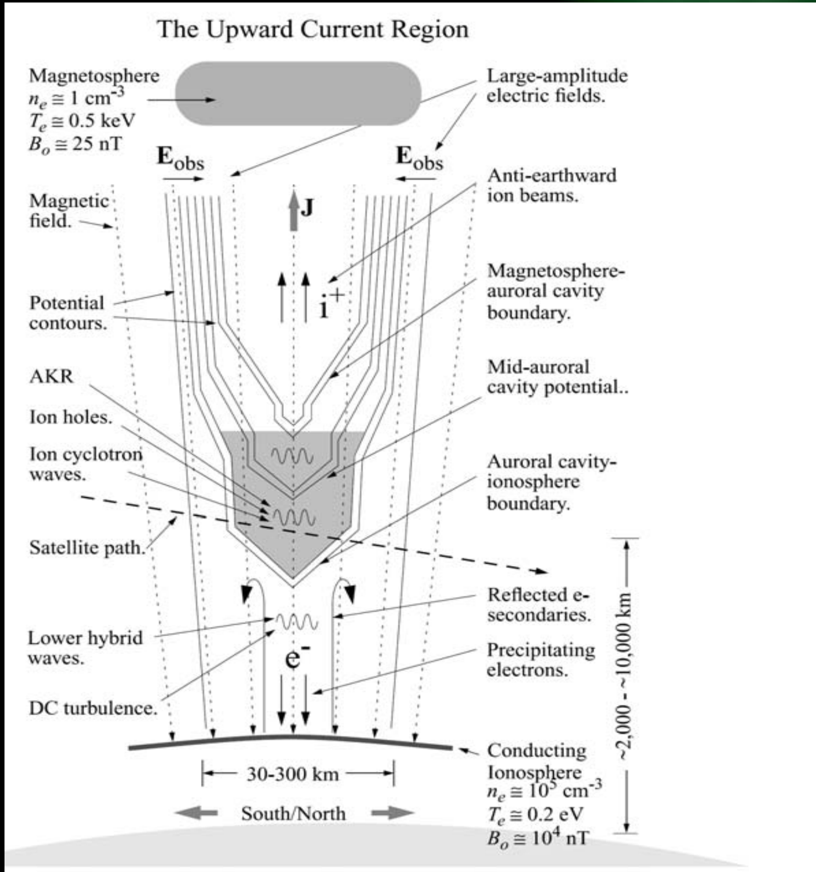


ed cartoon of the upward current region of the aurora. The potential conto
ltitude and high-altitude acceleration region with the auroral cavity in b

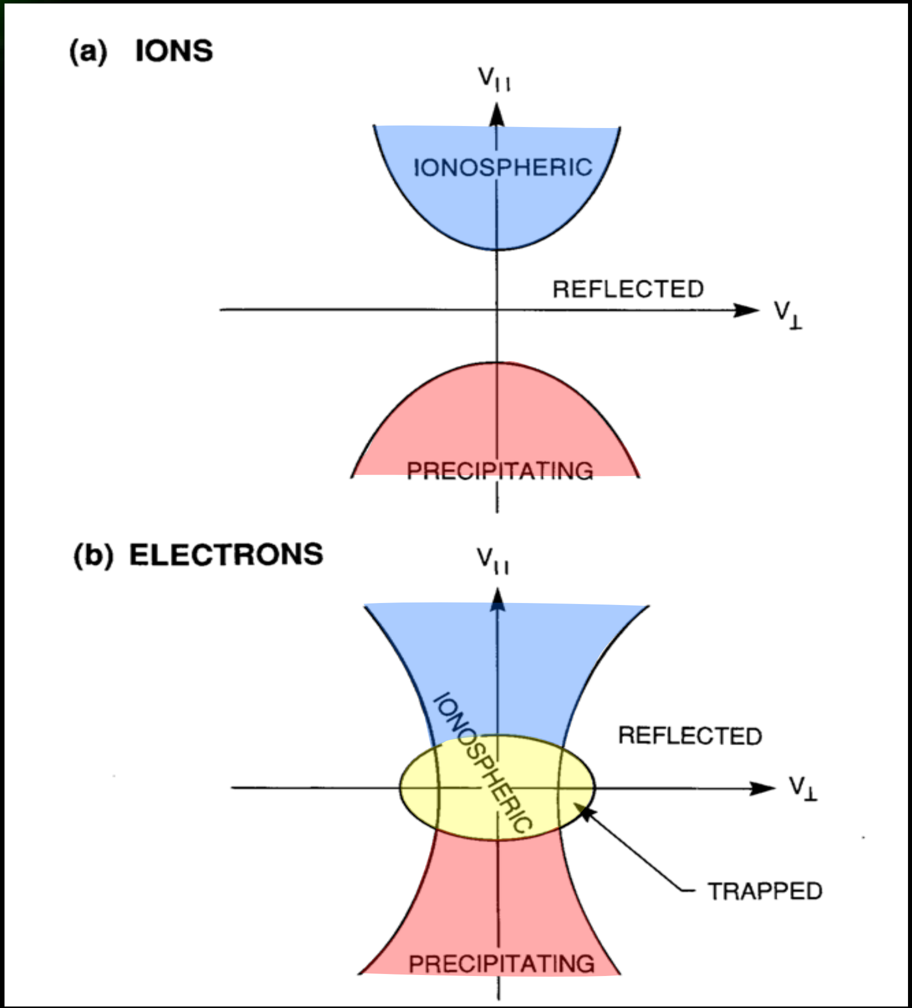

# Accelerated Maxwellian

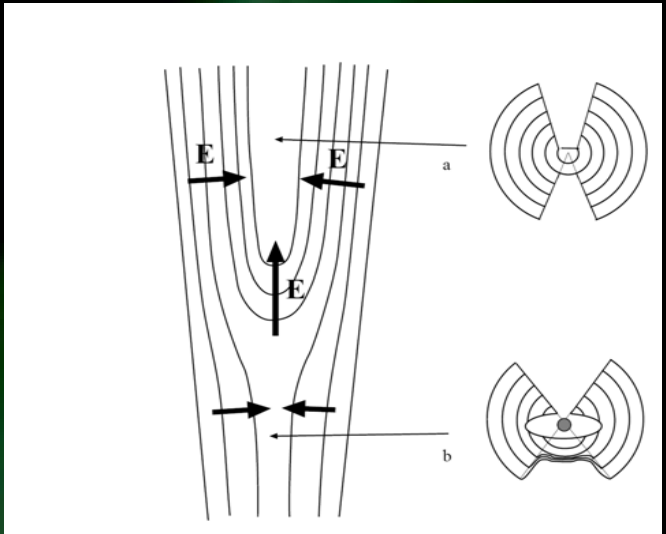


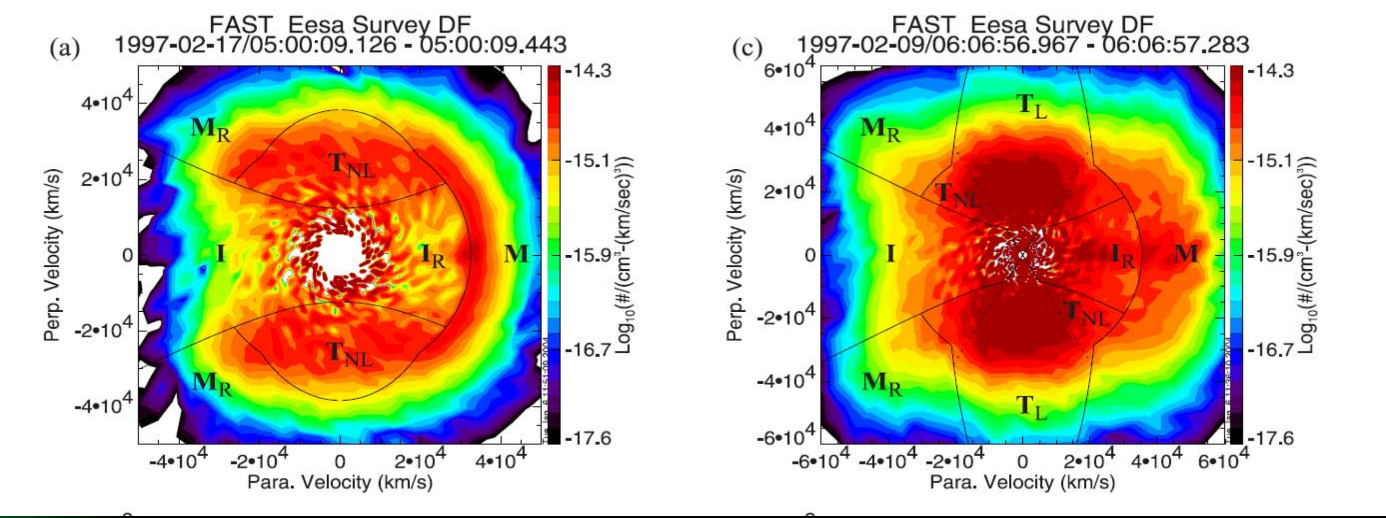

# Acceleration regions

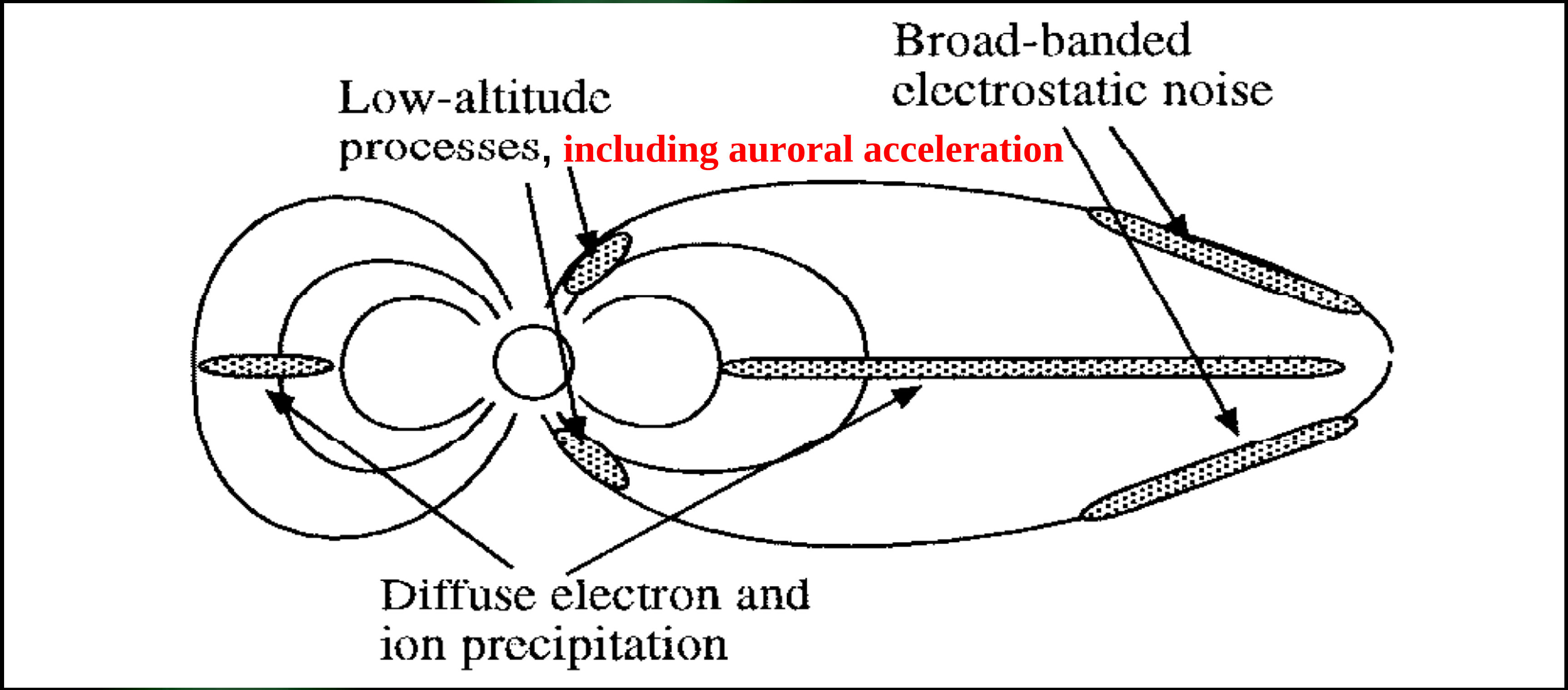


Koskinen

Auroral acceleration region typically situated at altitude of 1-3 $R_E$

# Mapping of auroral electric fields

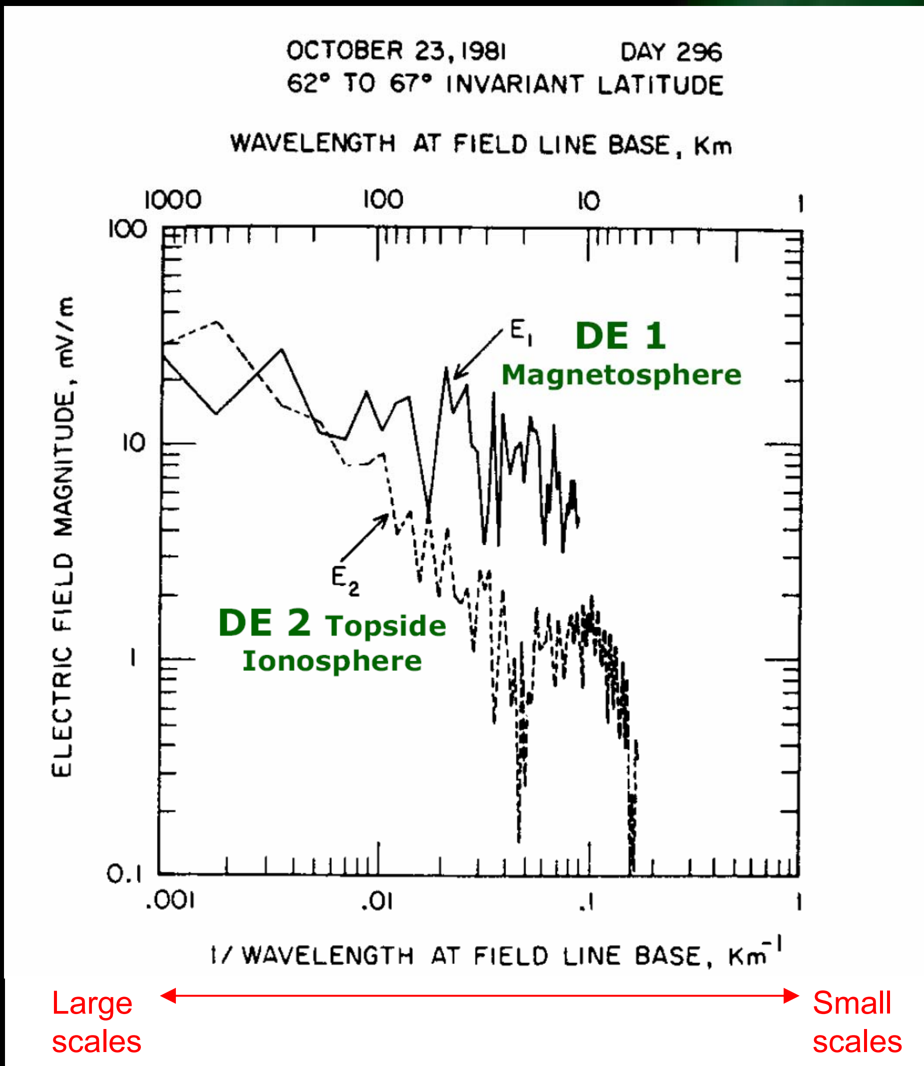


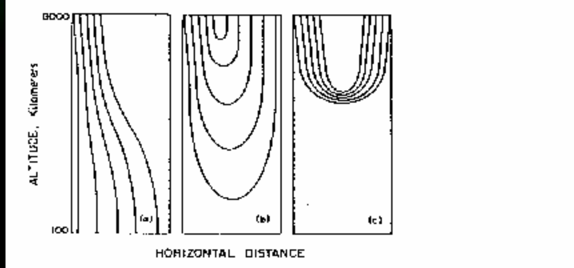


Figura 8. Contururi echipotentiale posibile in zona de accelerare (v. text). Din Hudson and Mozer (1978)

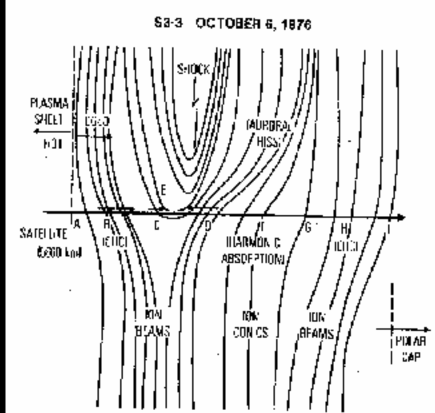


Figura 9. Reconstructia calitativa a contururilor echipotentiale din date S3-3. Figura ilustreaza 1 minut de observatii. Din Mizera et al. (1982)

Experimental results, comparison between Dynamics Explorer 1 and 2 at different altitudes. (*Weimer et al., 1985*)

# Static, medium-scale MI-coupling

MI-coupling critical scale size II

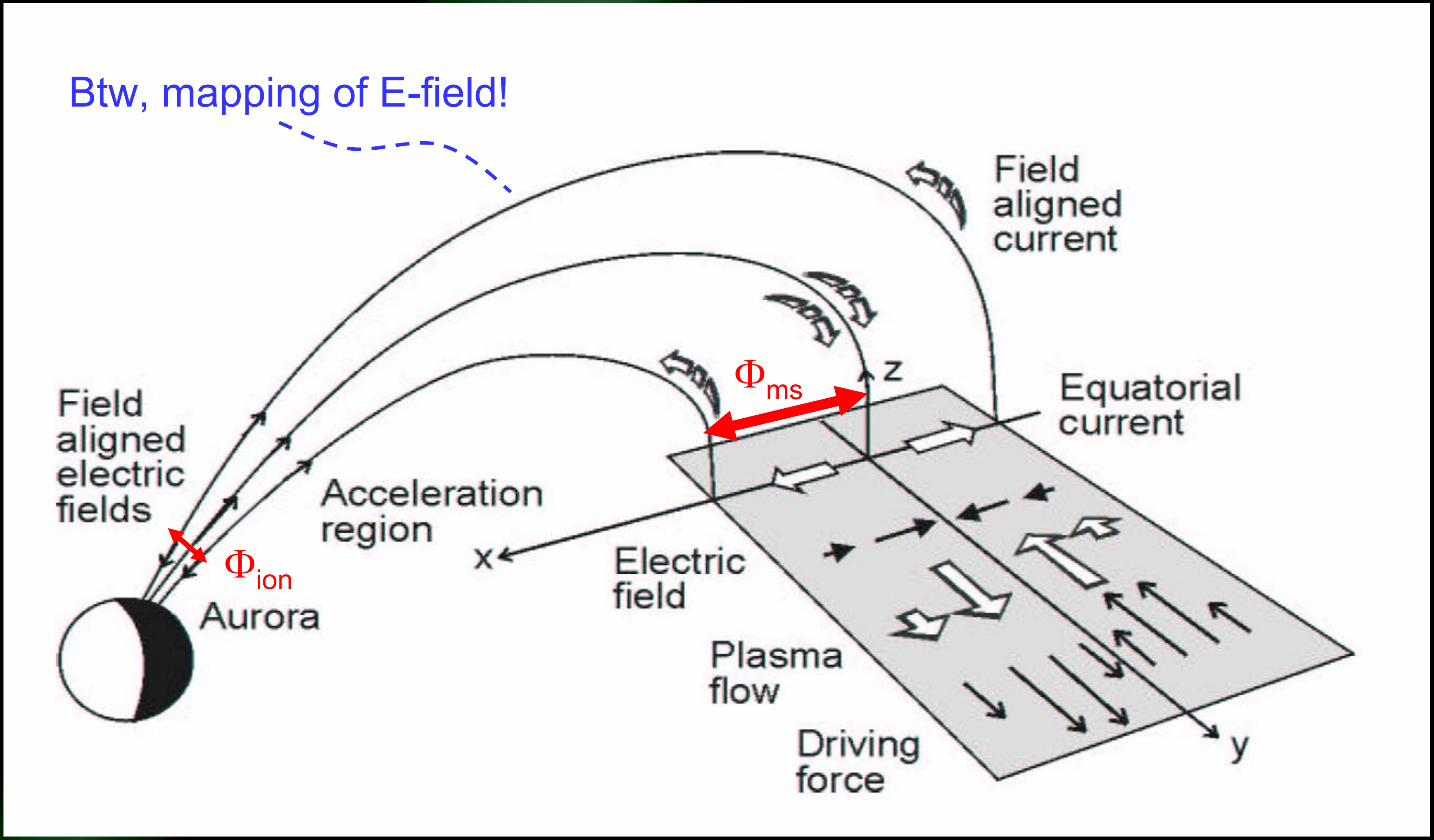

# Static, medium-scale MI-coupling

MI-coupling critical scale size III

$$j_{//} = \Sigma_P \nabla_\perp \cdot \mathbf{E}_\perp + \mathbf{E}_\perp \cdot \nabla_\perp \Sigma_P + (\mathbf{E}_\perp \times \nabla_\perp \Sigma_H) \cdot \hat{\mathbf{b}}$$

$$j_{//} = \Sigma_P \nabla_\perp \cdot \mathbf{E}_\perp$$

$$j_{||} = K \Delta\Phi_{//} = K(\Phi_{ms} - \Phi_{ion})$$

$$K(\Phi_{ms} - \Phi_{ion}) = \Sigma_P \nabla_\perp \cdot \mathbf{E}_{\perp ion}$$

$$K(\Phi_{ms} - \Phi_{ion}) = \Sigma_P \nabla_\perp^2 \Phi_{ion}$$

$$K(\Phi_{ms} - \Phi_{ion}) \approx \Sigma_P \frac{\Phi_{ion}}{L^2}$$

$$\Phi_{ion} = \left(1 + \frac{\Sigma_P}{KL^2}\right)^{-1} \Phi_{ms}$$

When L >> $\sqrt{\frac{\Sigma_P}{K}}$ : $\Phi_{ion} \approx \Phi_{ms}$

When L << $\sqrt{\frac{\Sigma_P}{K}}$ : $\Phi_{ion} \ll \Phi_{ms}$

The last case means $|\Phi_{ms}| \approx |\Delta\Phi_{//}|$

# Static, medium-scale MI-coupling

## MI-coupling critical scale size

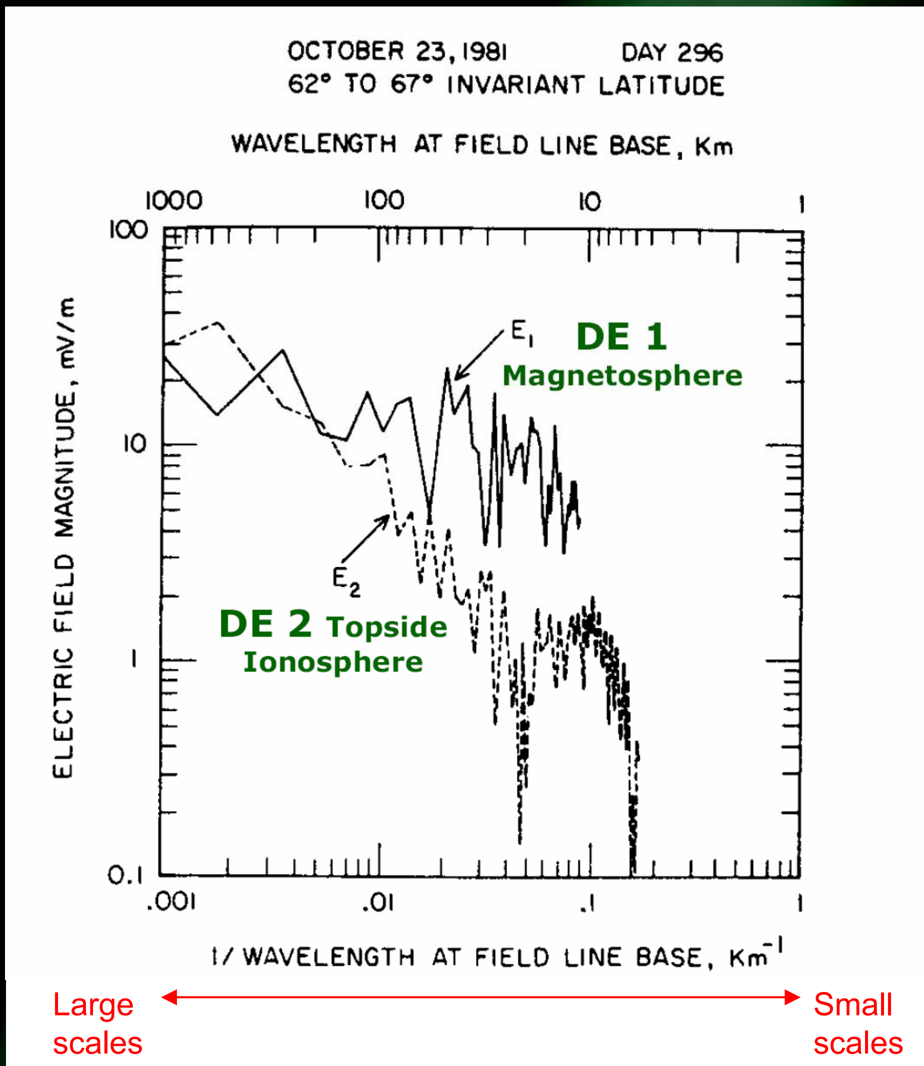


Experimental results, comparison between Dynamics Explorer 1 and 2 at different altitudes. (*Weimer et al., 1985*)

1/ WAVELENGTH AT FIELD LINE BASE, $Km^{-1}$

Fig. 4. Electric field spectrums from day 296 (October 23) of 1981. The spectrums are obtained from a Fourier transform of the electric field data between 62° and 67° invariant latitude. The solid line shows the spectrum of the electric field measured by DE 1. The solid line shows the spectrum of the electric field measured by DE 2. The ordinate values are obtained from the square root of the "spectral power density." The actual units are mV $m^{-1}$ $km^{1/2}$.

**Weimer et al, 1985**

# Downward current region

Upward current region

Downward electron beams: *Narrow in energy - broad in pitch-angle*

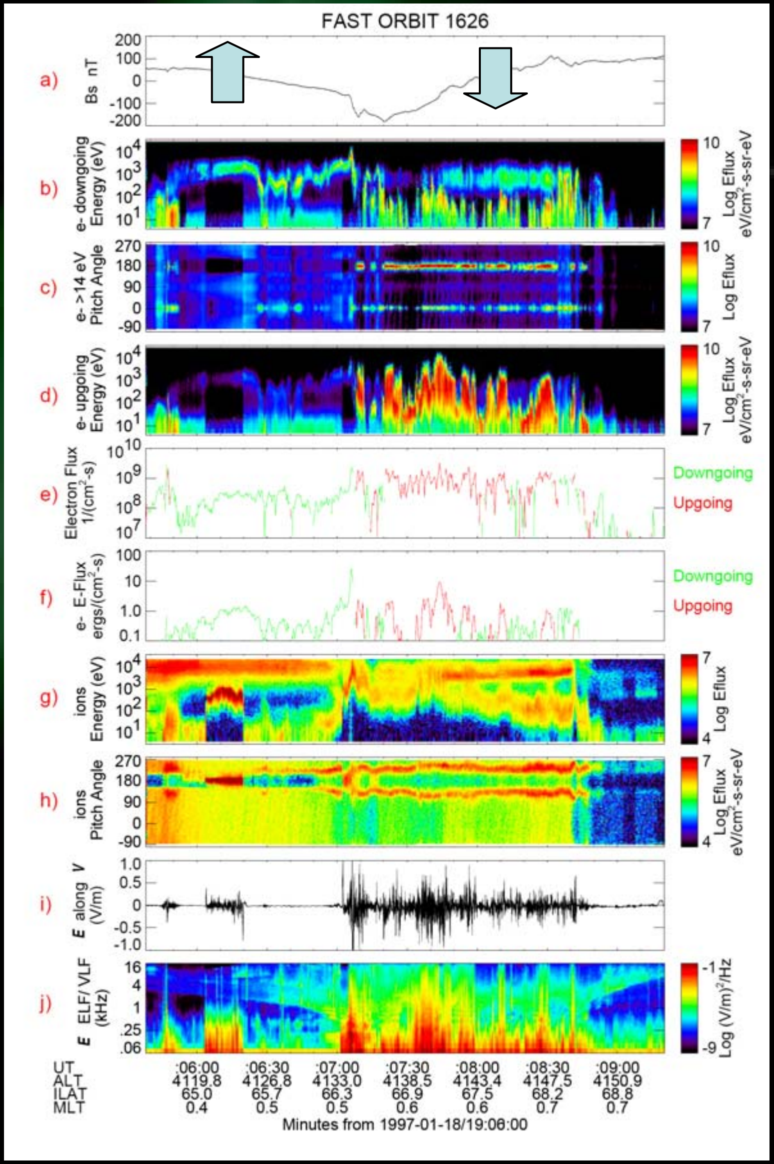


Downward current region

Upward electron beams: *Narrow in pitch angle - broad in energy*

# Upward electron beam

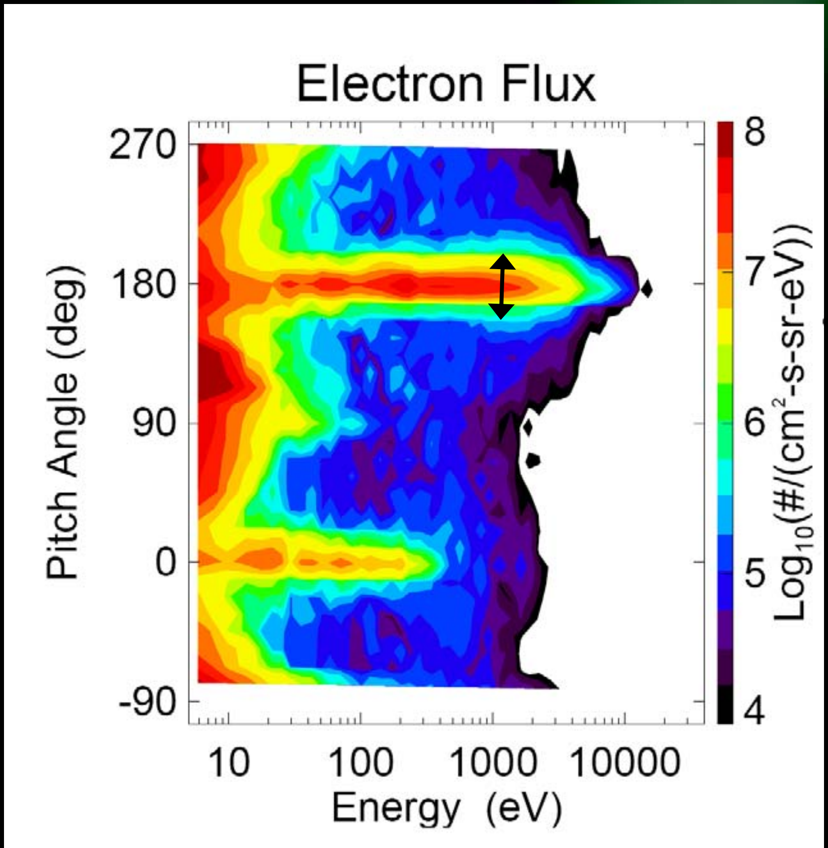


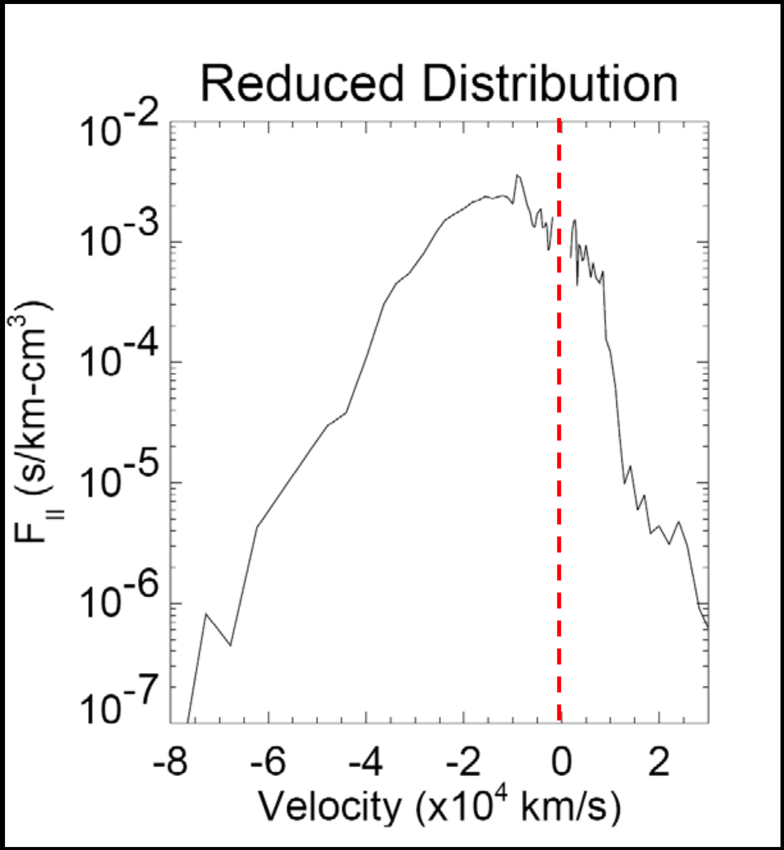


Seemingly also a downward beam?? But…

# Potential structure in the downward current region

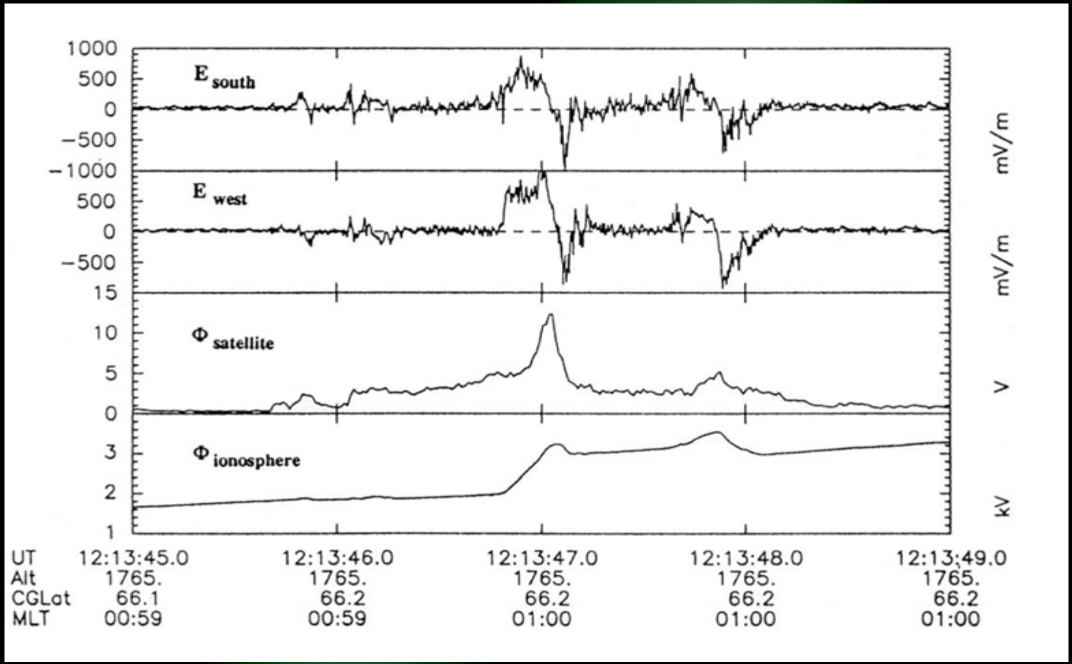


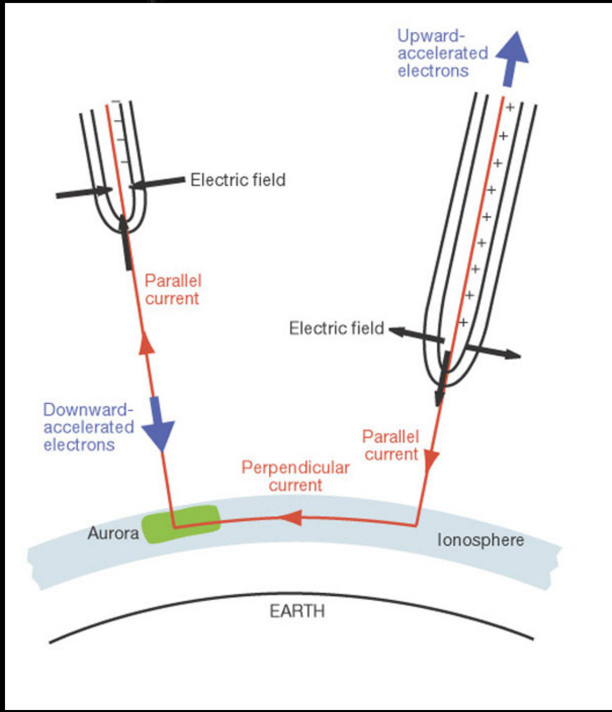


Freja electric field measurements, (Marklund et al., 1994)

# Upward electron beams

- Good agreement with integrated E-field
- Widening in energy is due to extensive wave-particle interaction.

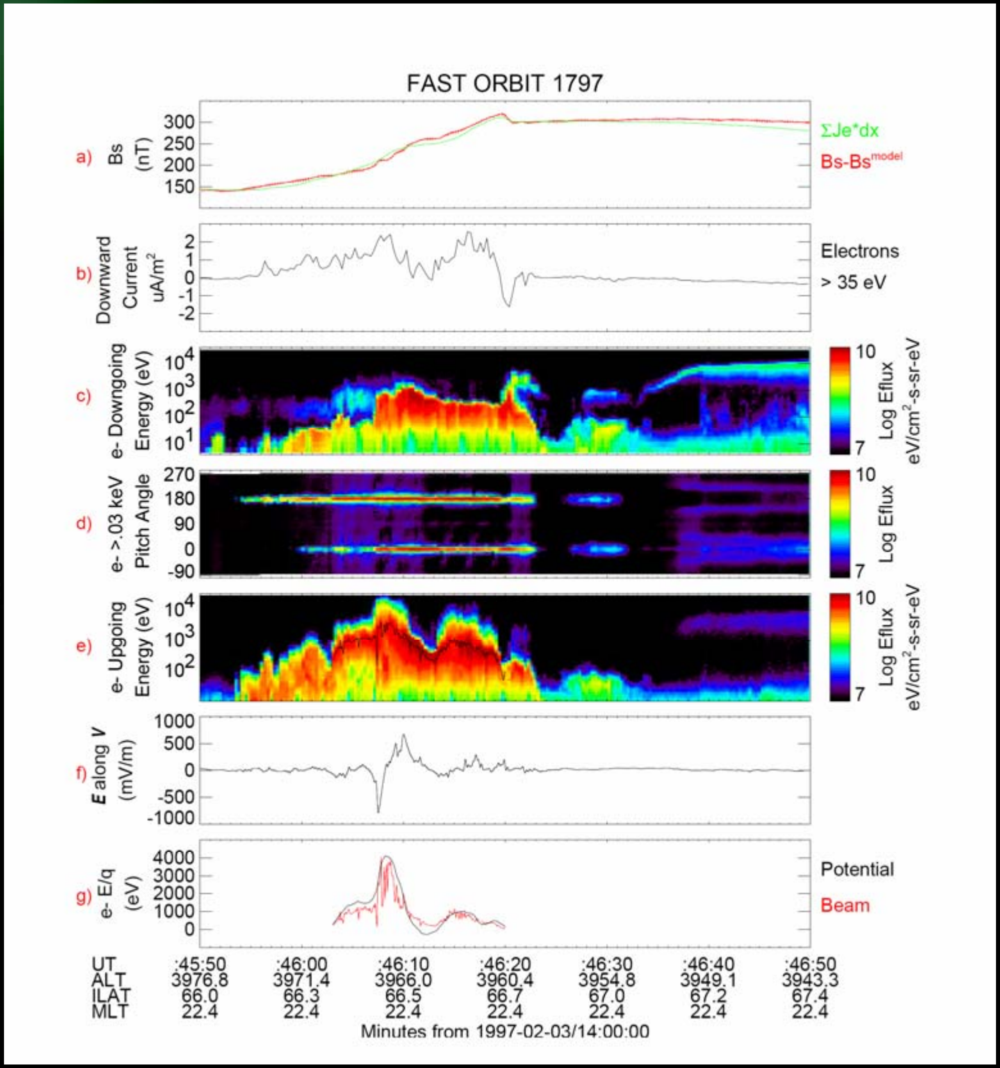

# Ion conics and beams

## ‘Distribution functions’

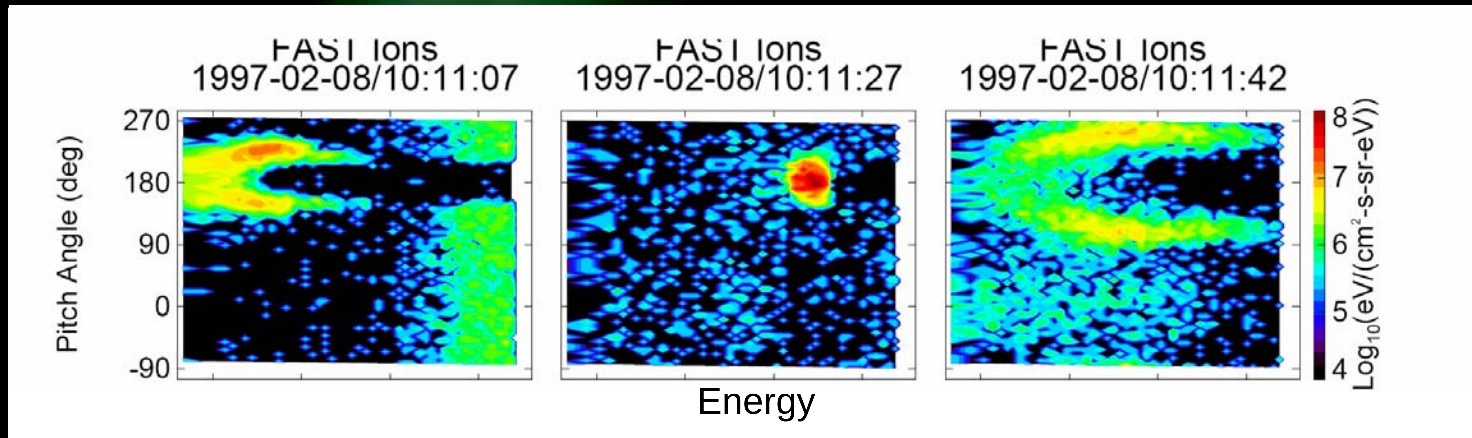


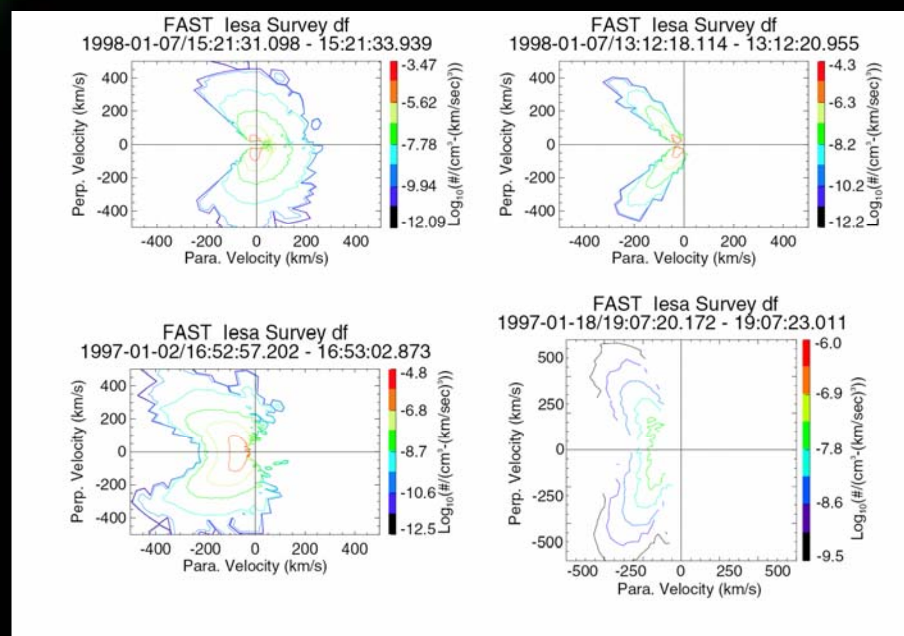

# Ion conics – adiabatic motion

In a sense the opposite process to magnetic mirroring

$$\mu = \frac{mv_{\perp}^{2}}{2B} = \frac{mv^{2}\sin^{2}\alpha}{2B}$$

Magnetic moment conserved

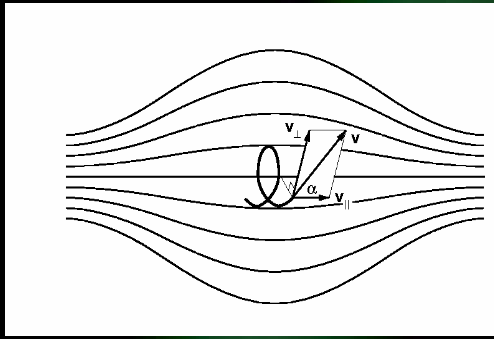


Weaker B means α decreases

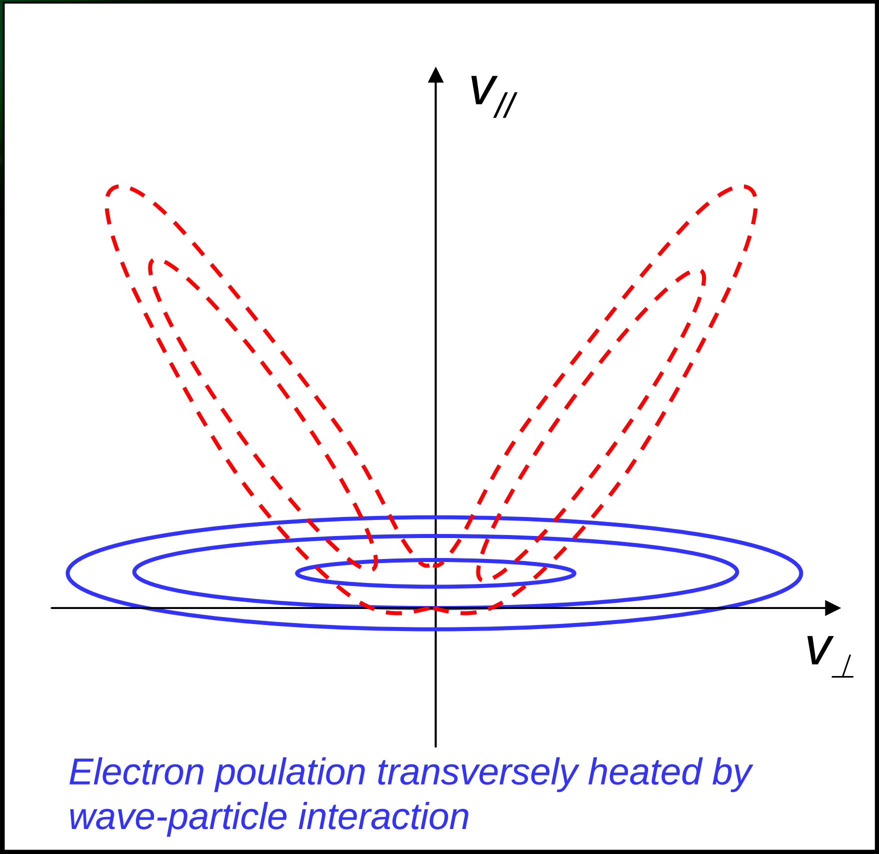


An ion distribution originally heated in the direction perpendicular to B will fold up to a conic

$$\alpha = \sin^{-1}\sqrt{\frac{B}{B_0}}$$

# Ion conics

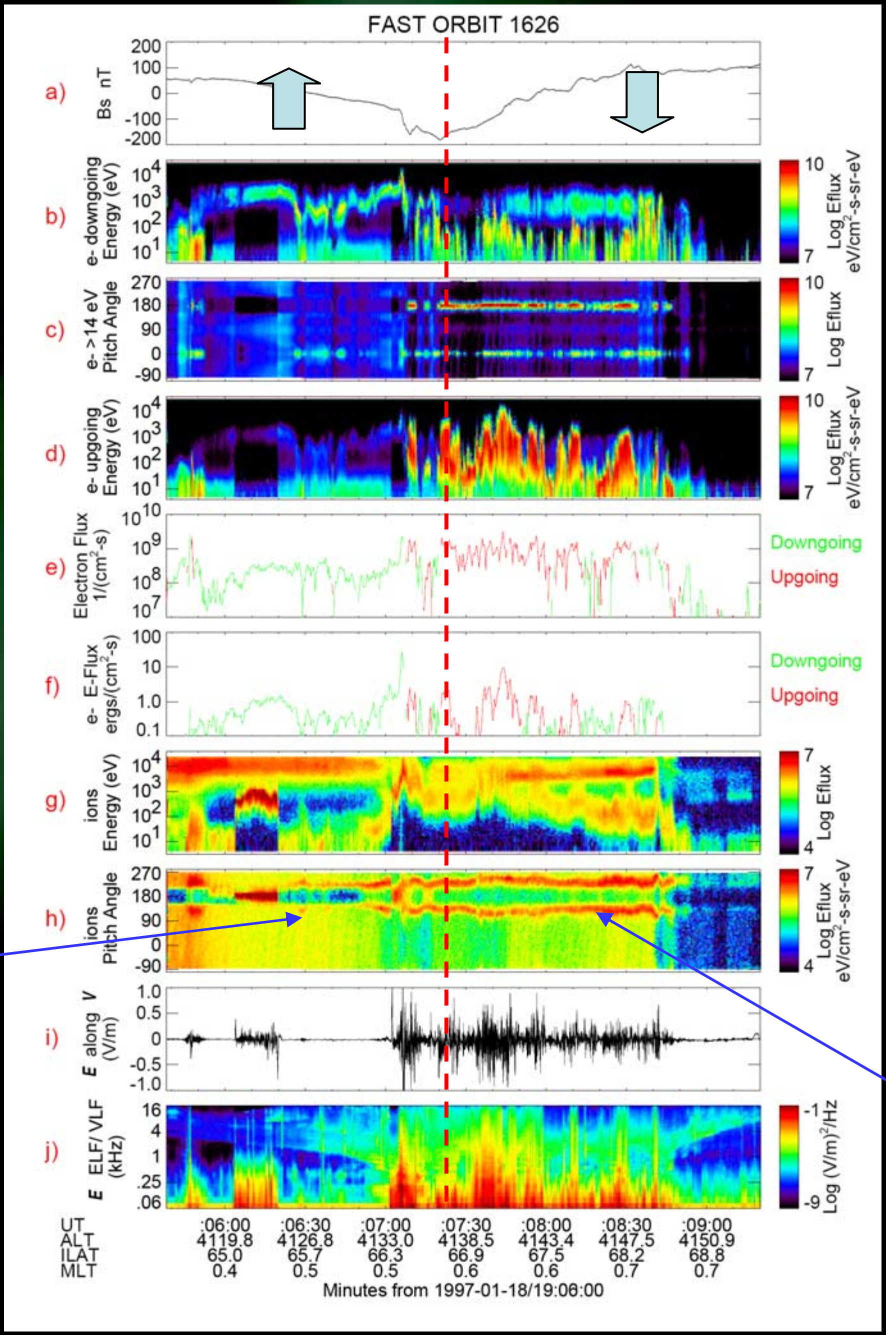

FAST ORBIT 1626
a) Bs nT
b) e- downgoing Energy (eV)
Log Eflux eV/cm2-s-sr-eV
c) e- >14 eV Pitch Angle
Log Eflux
d) e- upgoing Energy (eV)
Log Eflux eV/cm2-s-sr-eV
e) Electron Flux 1/(cm2-s)
Downgoing
Upgoing
f) e- E-Flux ergs/(cm2-s)
Downgoing
Upgoing
g) ions Energy (eV)
Log Eflux
h) ions Pitch Angle
Log Eflux eV/cm2-s-sr-eV
i) E along V (V/m)
j) E ELF/ VLF (kHz)
Log (V/m)2/Hz
UT :06:00 :06:30 :07:00 :07:30 :08:00 :08:30 :09:00
ALT 4119.8 4126.8 4133.0 4138.5 4143.4 4147.5 4150.9
ILAT 65.0 65.7 66.3 66.9 67.5 68.2 68.8
MLT 0.4 0.5 0.5 0.6 0.6 0.7 0.7
Minutes from 1997-01-18/19:06:00

# Ion conics – adiabatic motion

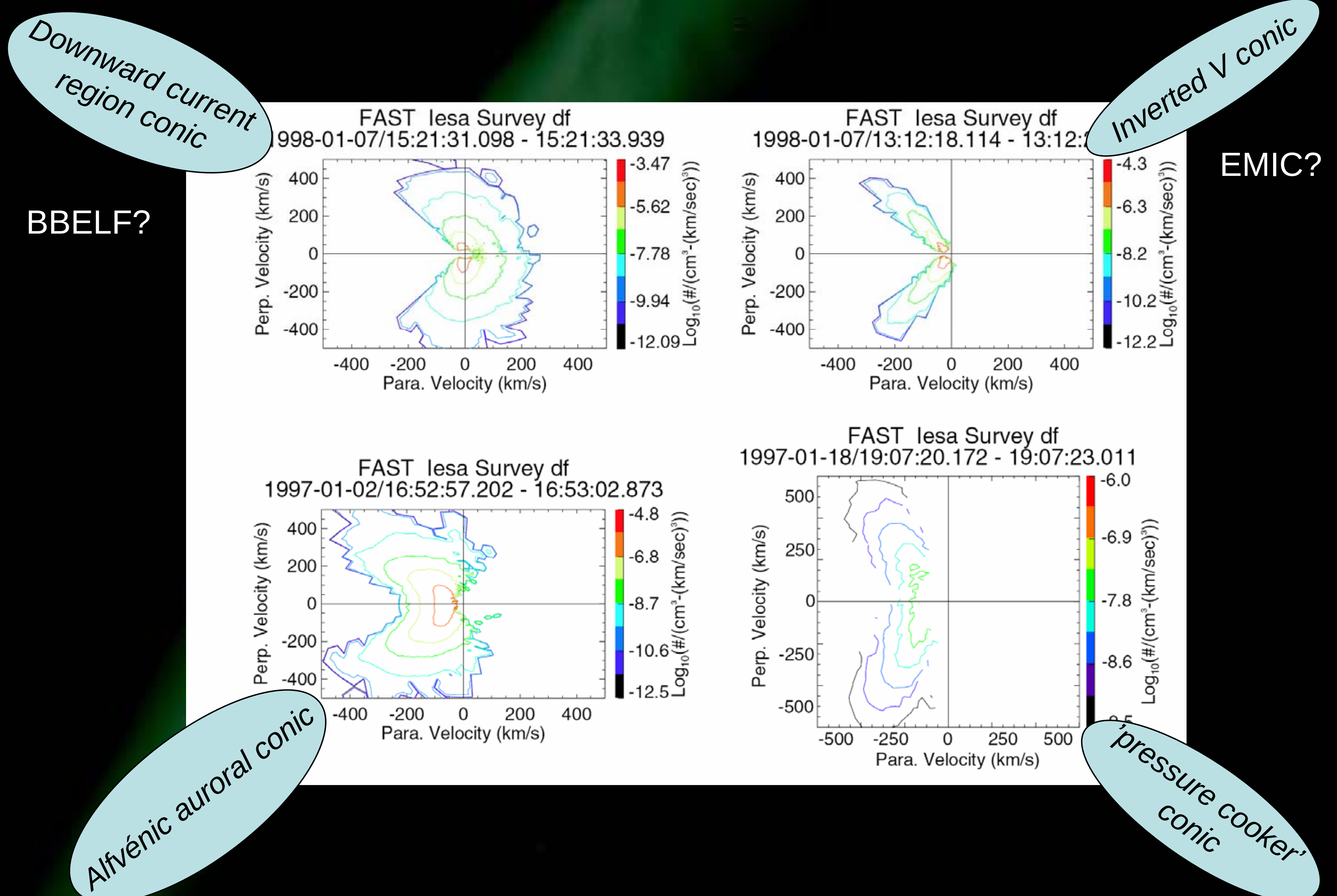

# Waves in upward current region

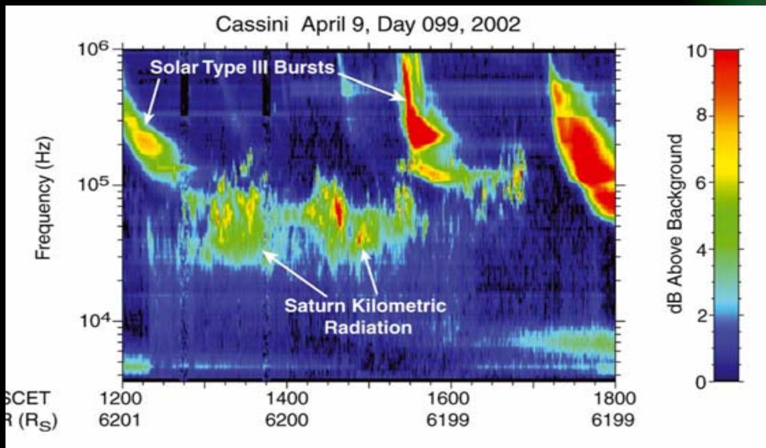


Saturn kilometric radiation

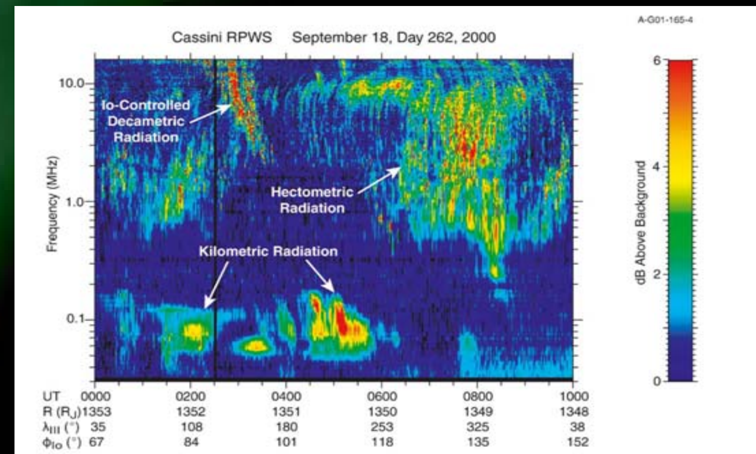


Jupiter hectometric radiation

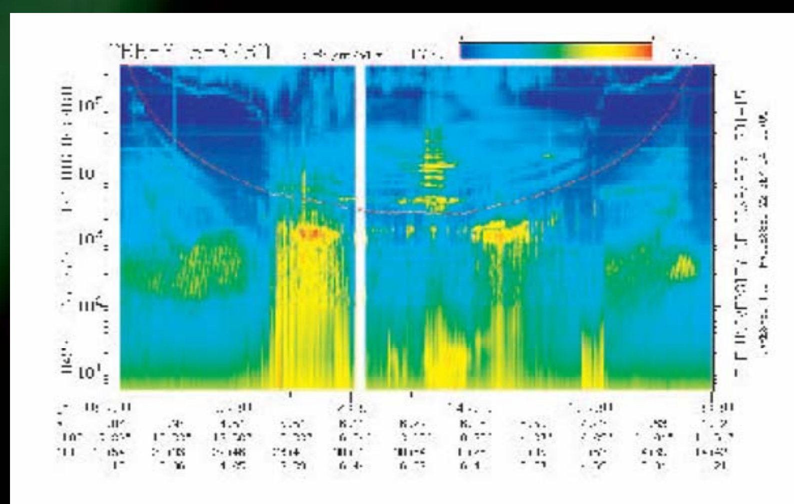

Auroral kilometric radiation

# Auroral kilometric radiation

Dominating radiative feature of auroral zone

Generated by cyclotron-maser instability in auroral acceleration region

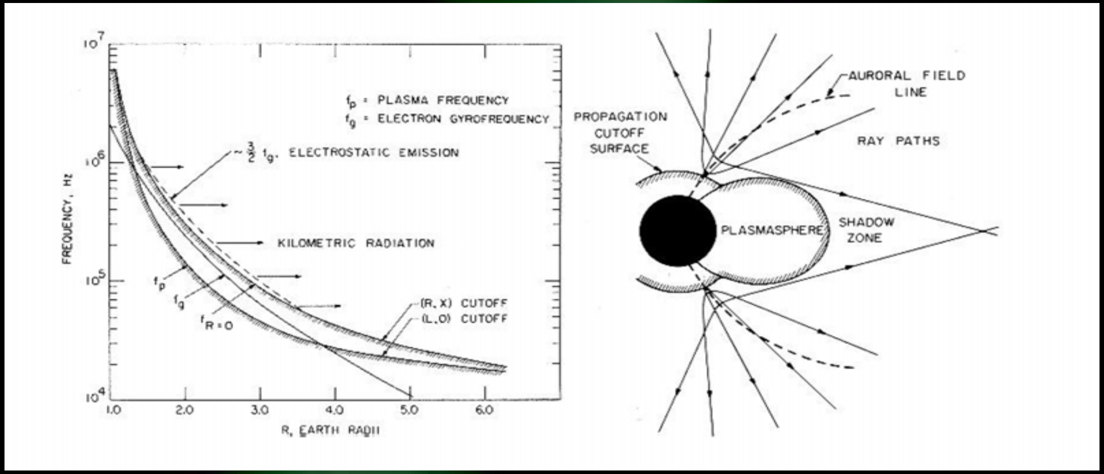


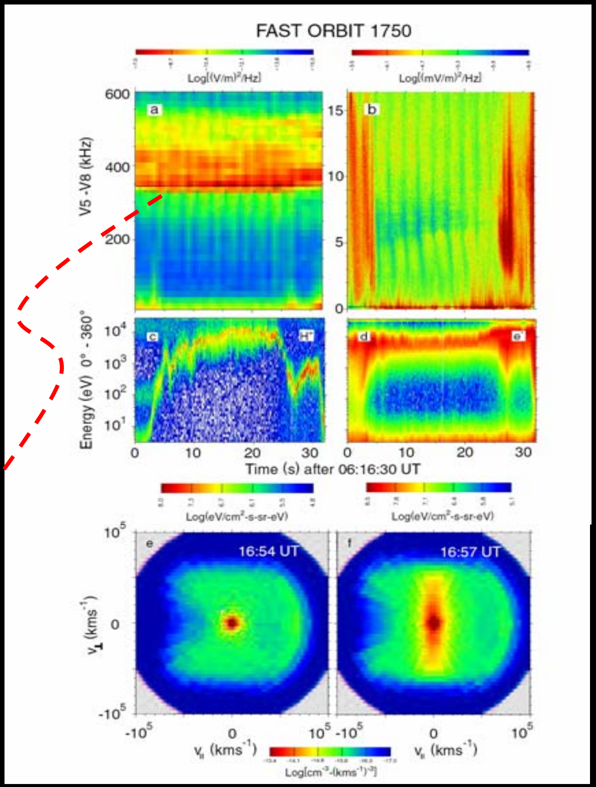


Lower cutoff at $\omega_{ce}$ of the *source region*.

# Waves in downward current region

## VLF saucers

- Often most prominent wave feature of downward current region.
- ***k*** larger angle for higher frequencies
- Probably generated by upward ion beams

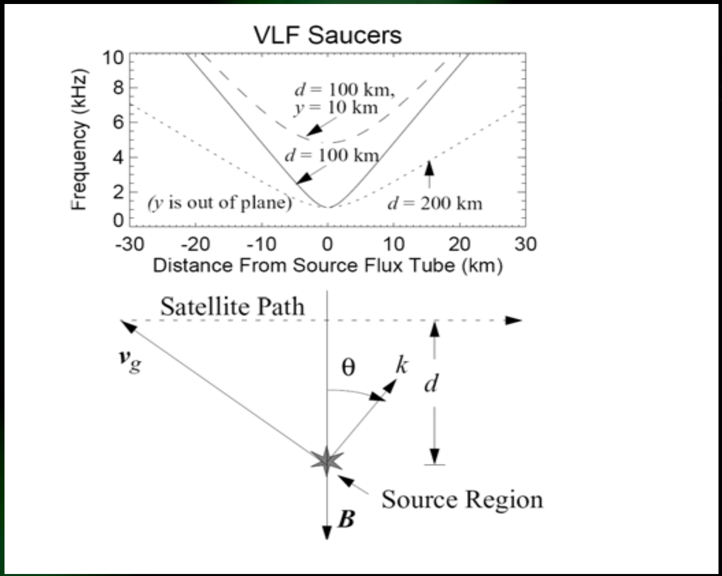


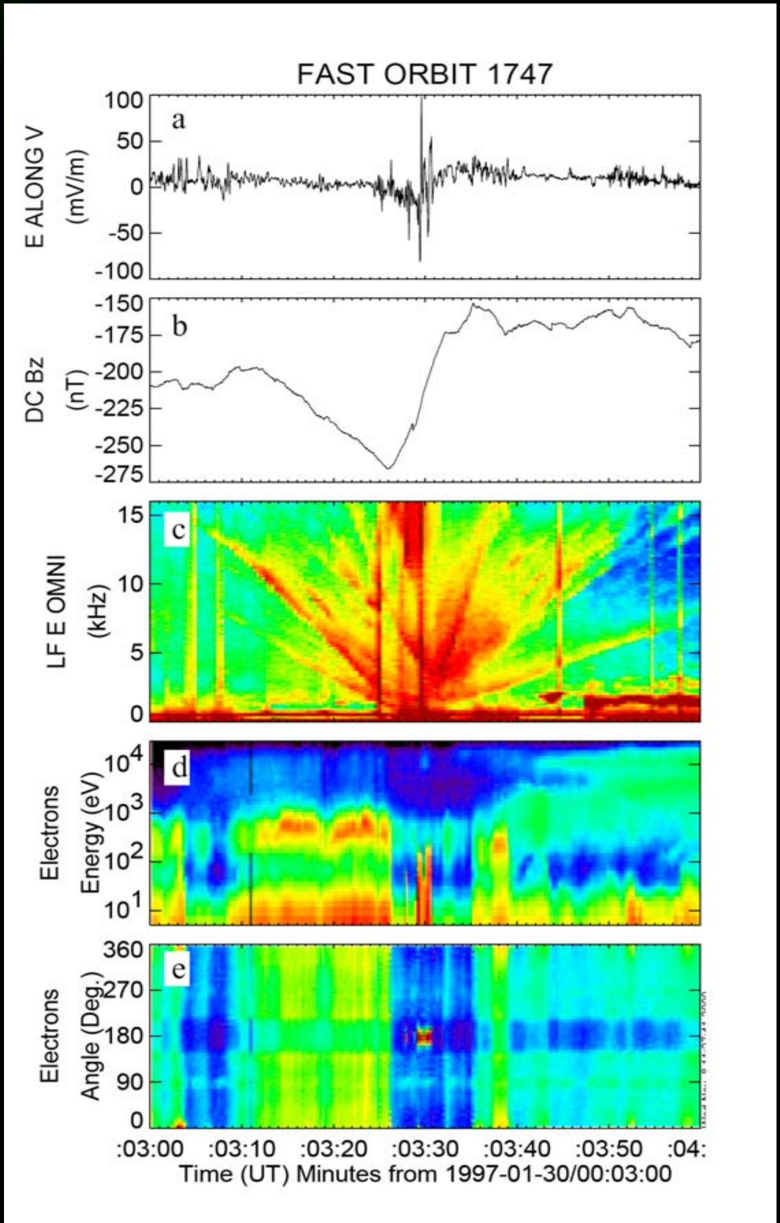

# The symmetry between the upward and downward current regions

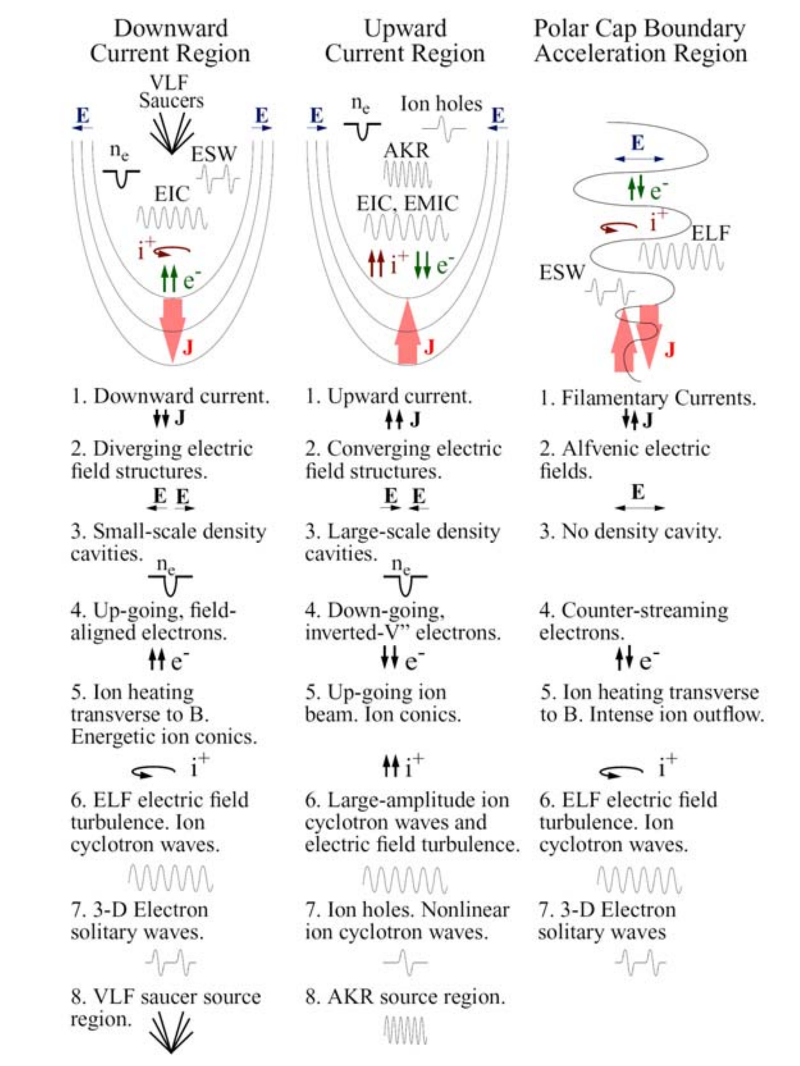


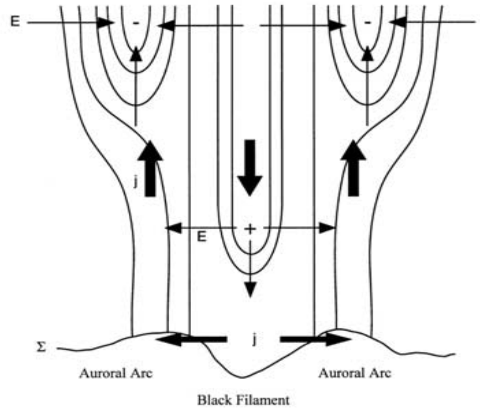

# Dynamic MI-coupling

## Alfvén wave driven aurora

*X-line aurora*

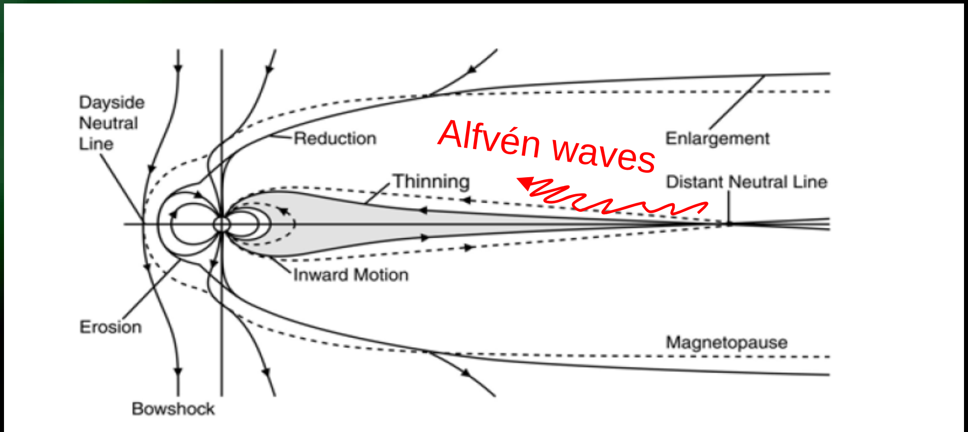


*Field-line resonances*

*Ionospheric auroral resonator*

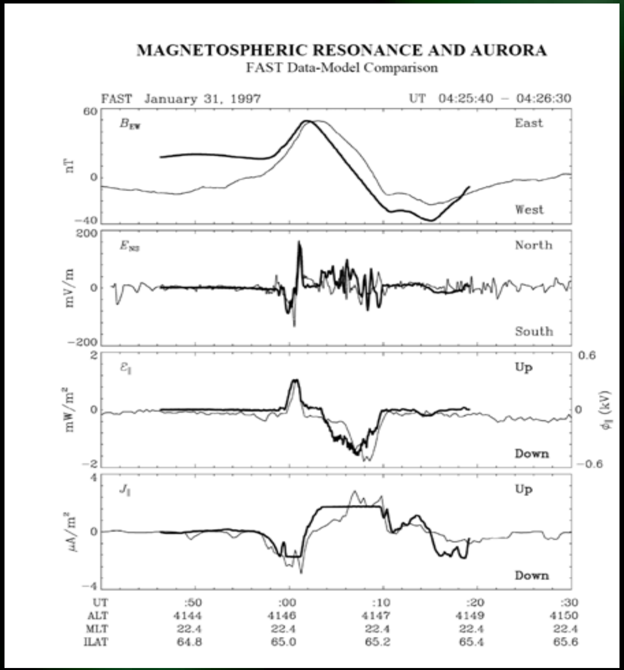


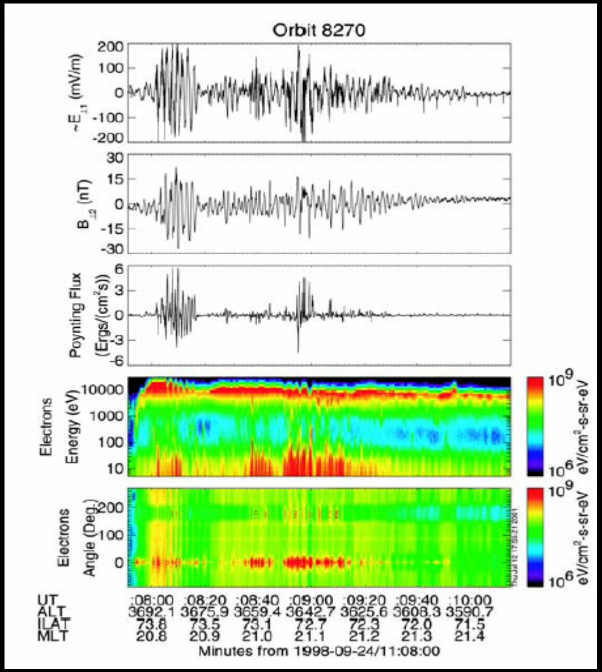


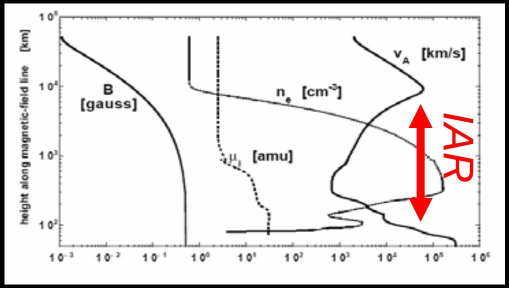


*Lotko et al., 1998*

*Chaston et al., 1999*

# Cusp and dayside aurora

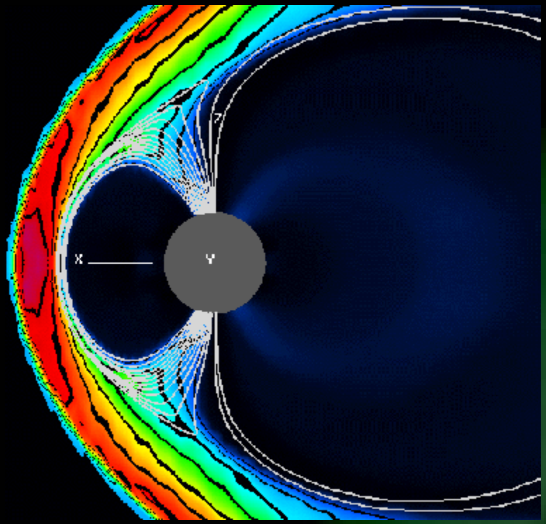

Direct entry of magnetosheath plasma
Fedder et al. (1997)

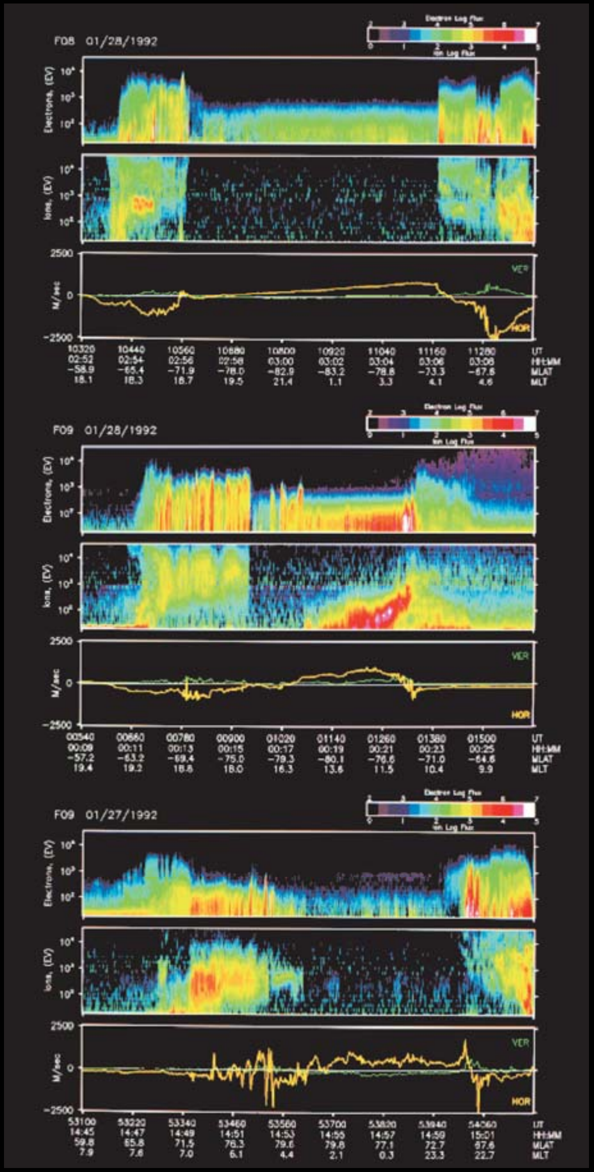


Velocity filter effect

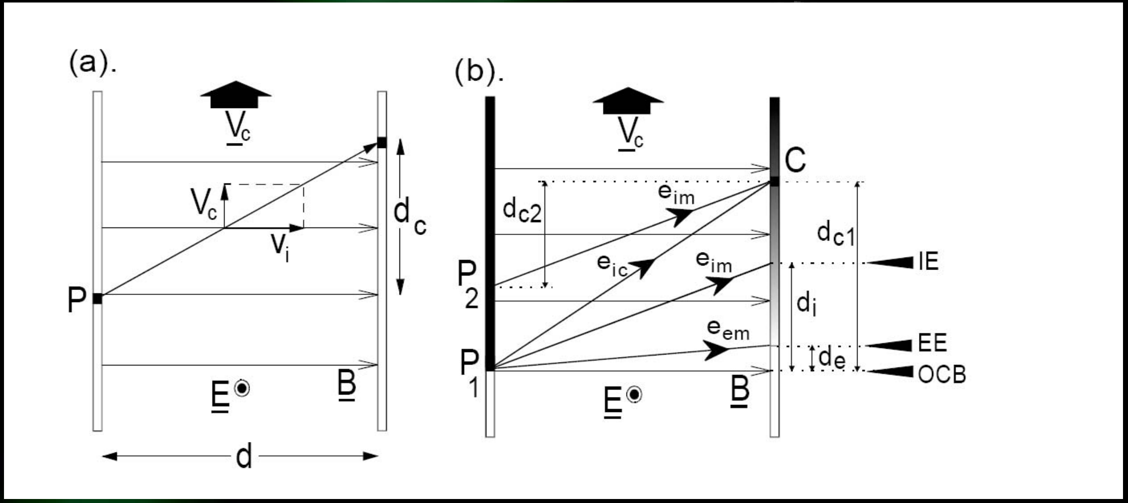


DMSP 9 data (Lyons et al., 1999)

# Theta aurora

What are they???

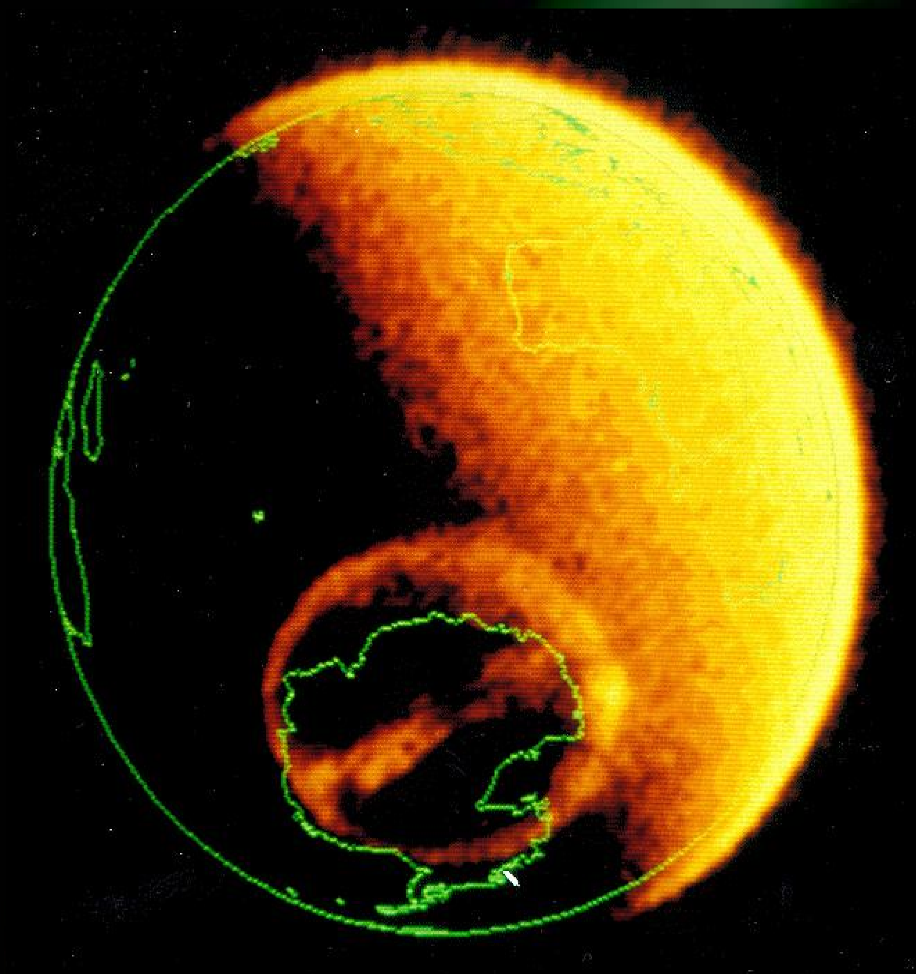

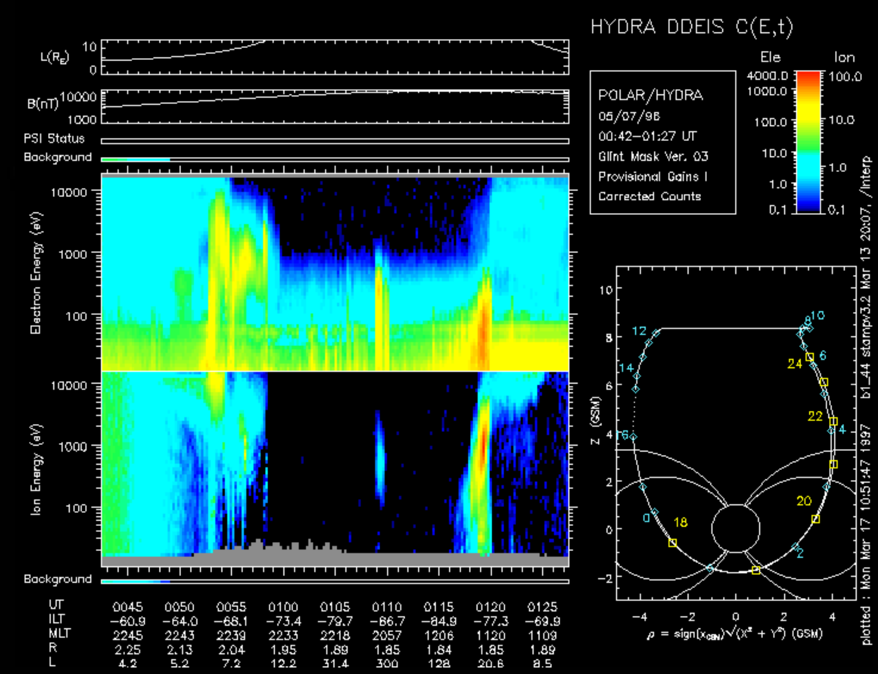

# Cluster multi-point measurements

## Seeing the temporal evolution

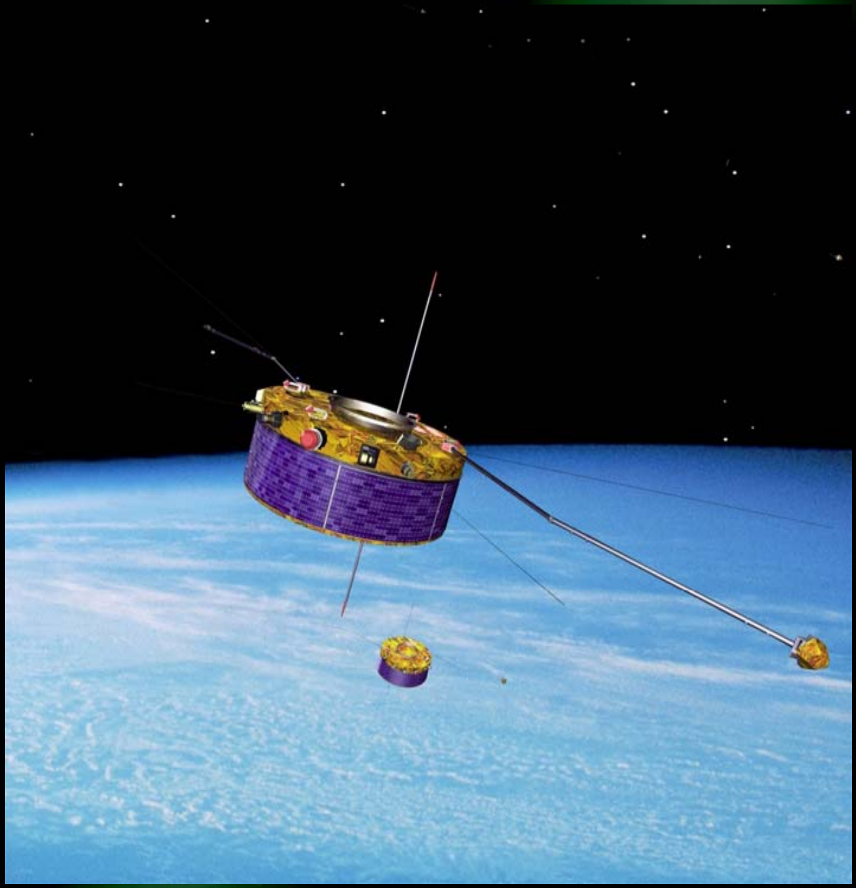

- Launched 2000
- Apogee: 20 $R_E$
- Perigee: 4 $R_E$
- Separations:
  200-10000 km

# Interpreting Cluster multipoint measurements

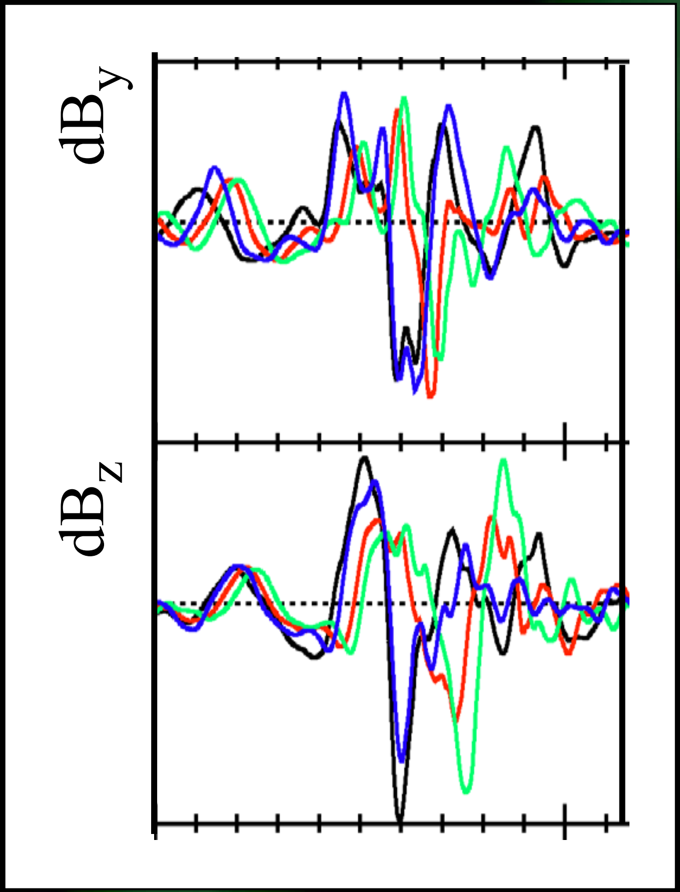


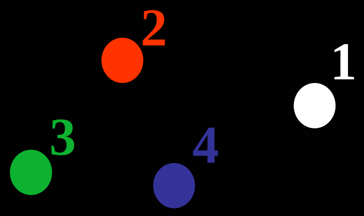

# Cluster field data

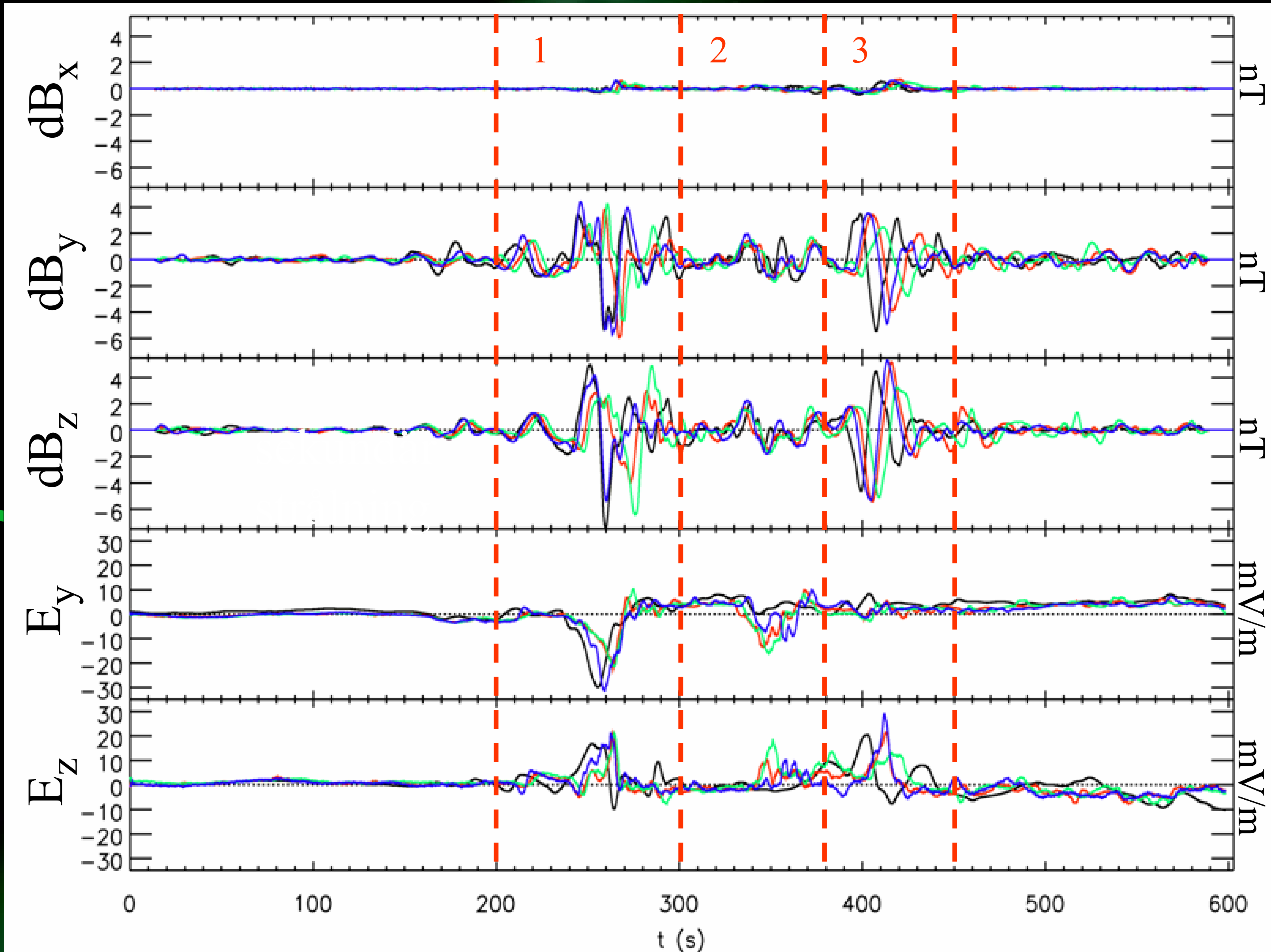

# CLUSTER multipoint measurements (1)

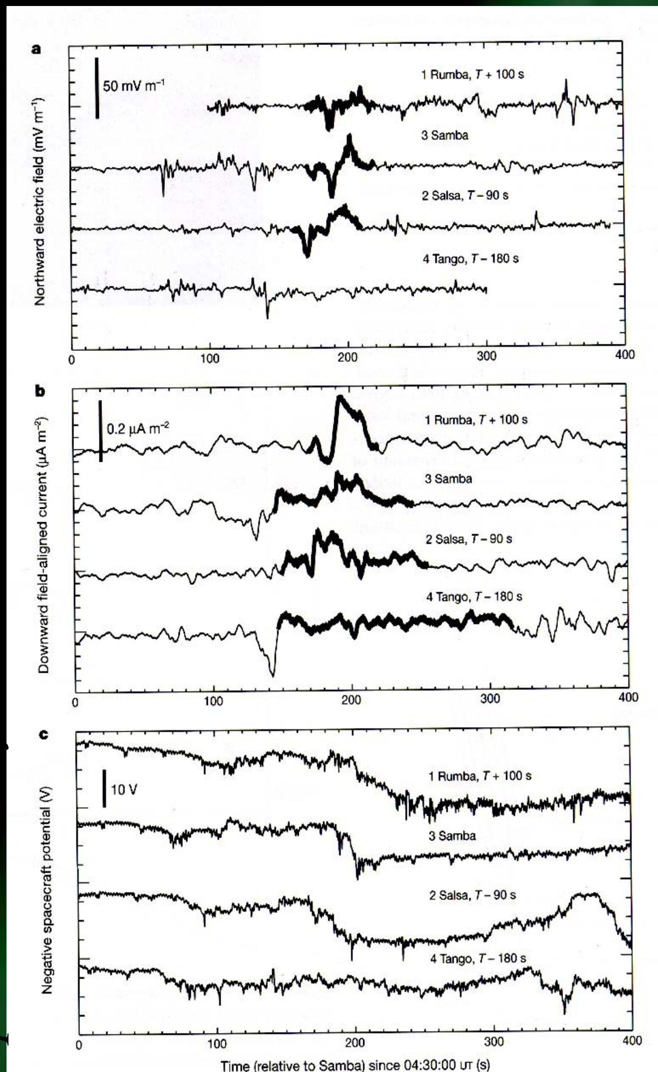


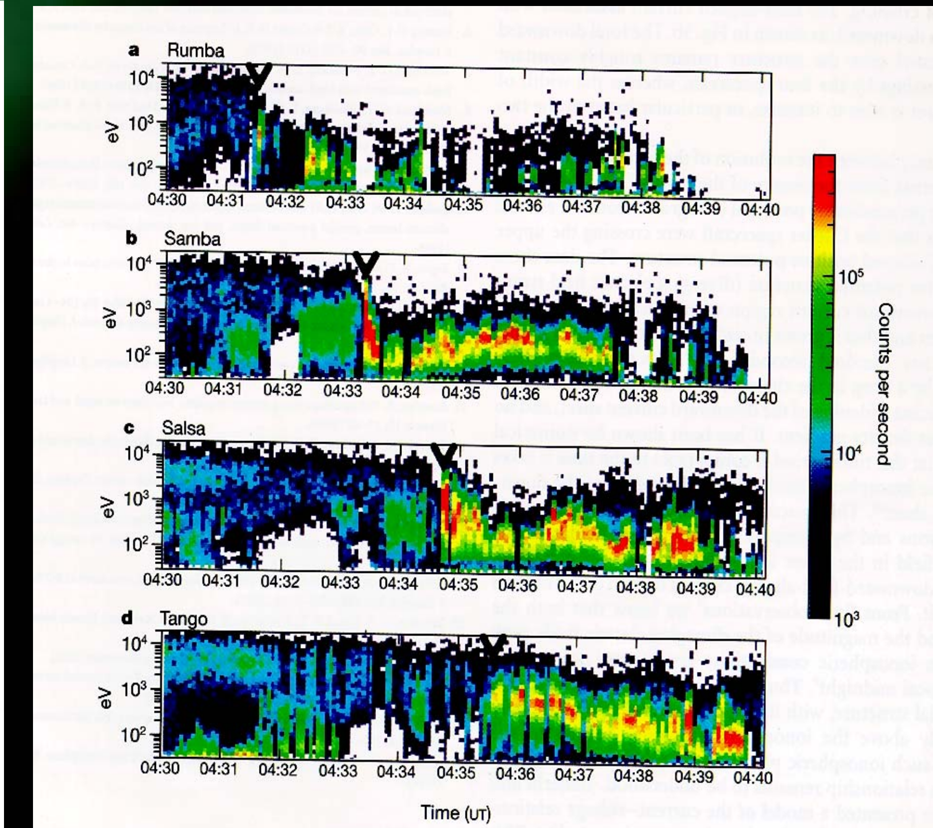


Marklund et al, 2001

# Cluster passage through black aurora

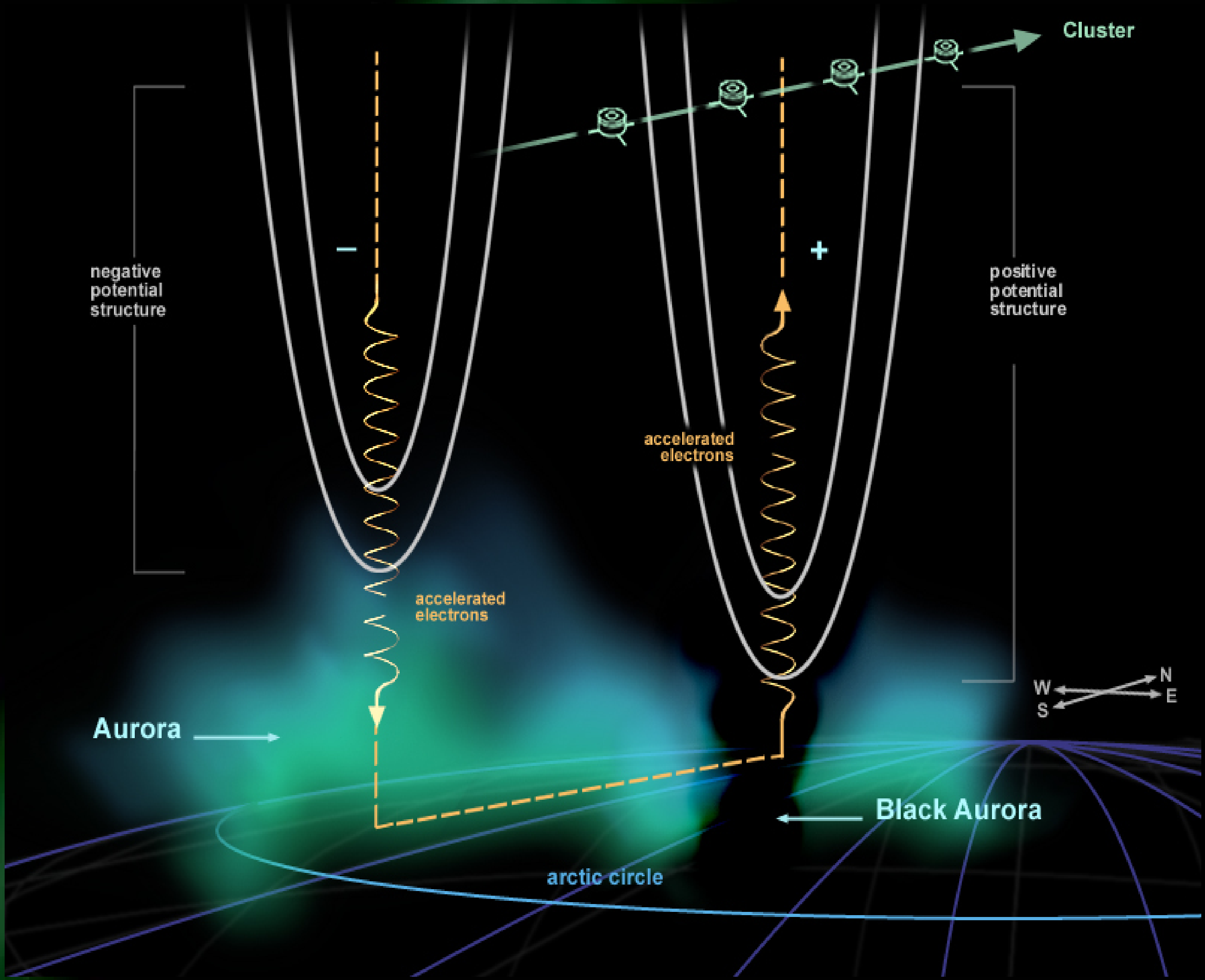

# Temporal evolution of the acceleration potential above black aurora

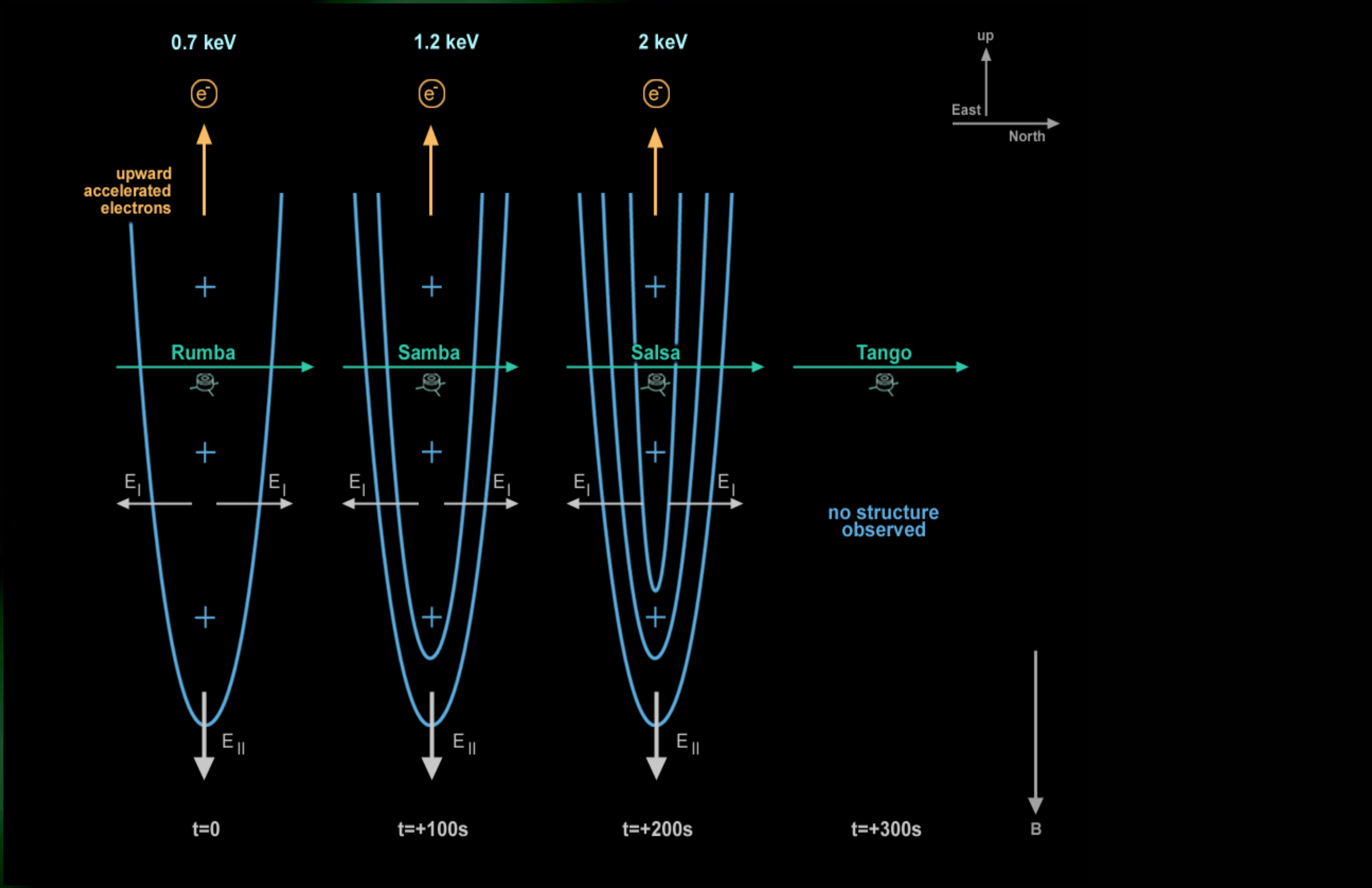

# The active role of the ionosphere

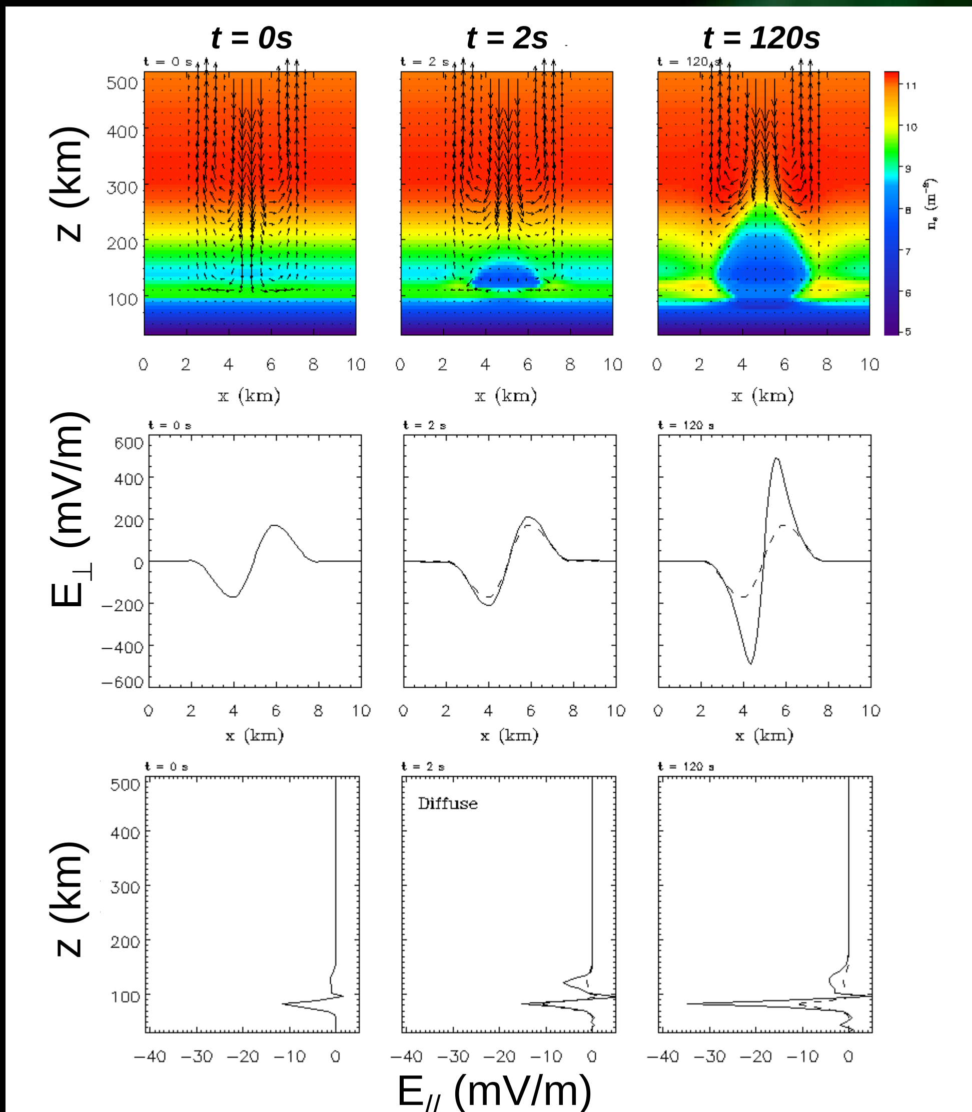


Karlsson, 1998

## Density cavities

*Simulations show deep density cavities formed by downward FAC and associated increased E-fields.*

*Important to take into consideration when mapping from high-altitude measurements.*

**Assumptions:**

**$j_{//}$ carried by $e^-$**
**$j_P$ carried by ions**

⇨

$$\frac{\partial n_e}{\partial t} = -\frac{1}{q}\frac{\partial j_{//}}{\partial z}$$

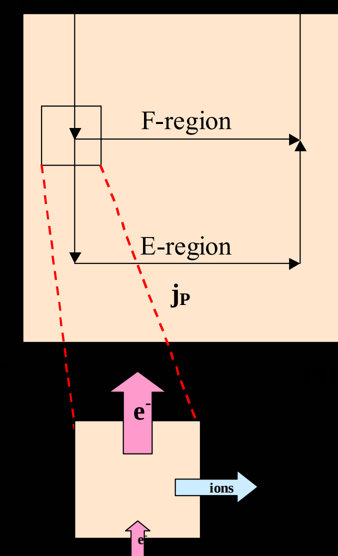

# Cluster data, 2004-02-18, and model results

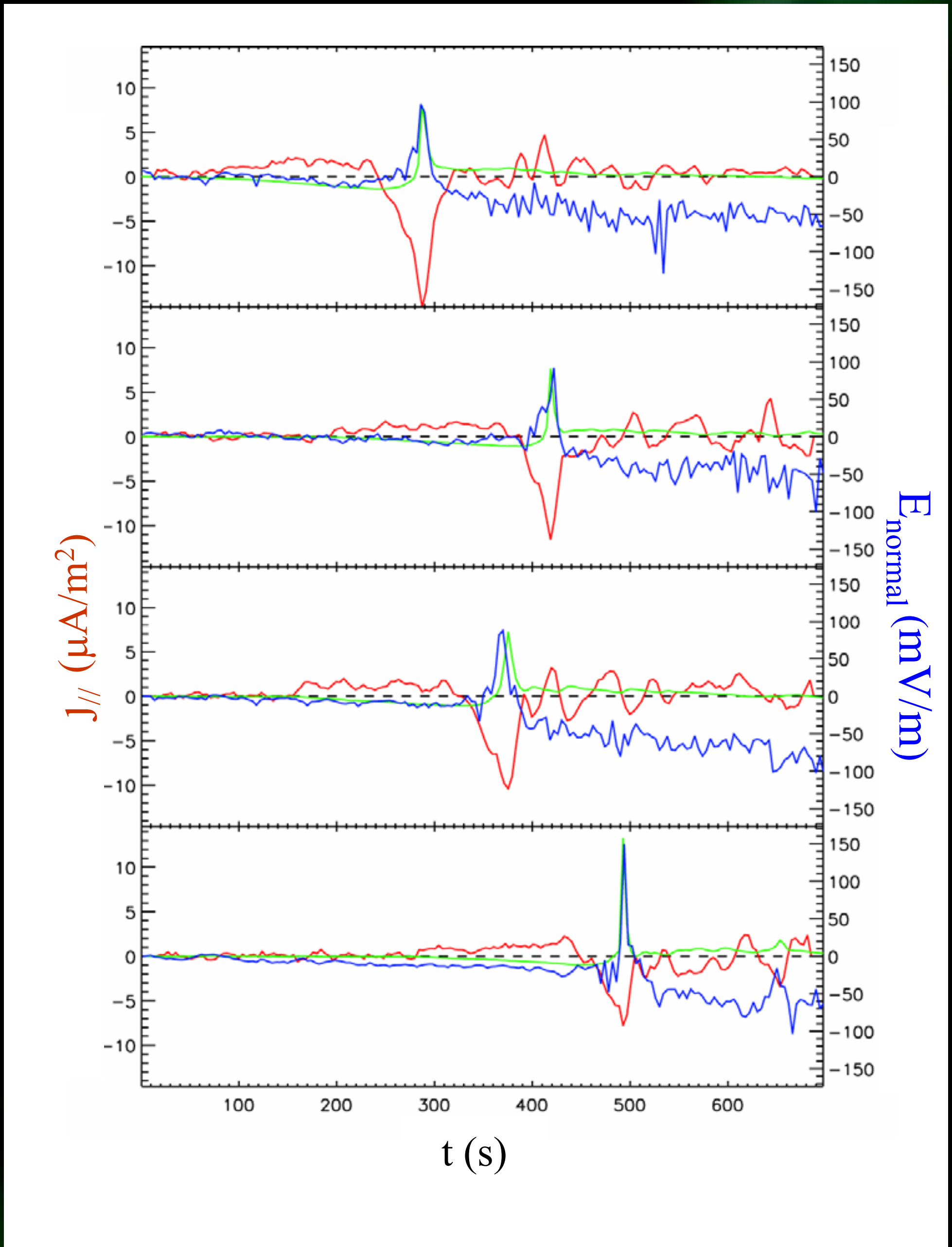


S/C 1-4
NH, MLT≈4, ILAT ≈~66

$E_n$ = 1 mV/m
$E_t$ = -3 mV/m
$\Sigma_{P,BG}$ = 5 S

$k_{down,1}$ = 0.31 Sm²/μA
$k_{down,2}$ = 0.40 Sm²/μA
$k_{down,3}$ = 0.42 Sm²/μA
$k_{down,4}$ = 0.72 Sm²/μA

*Karlsson, 2007*

# Model – inospheric modification by downward FAC

From earlier simulations

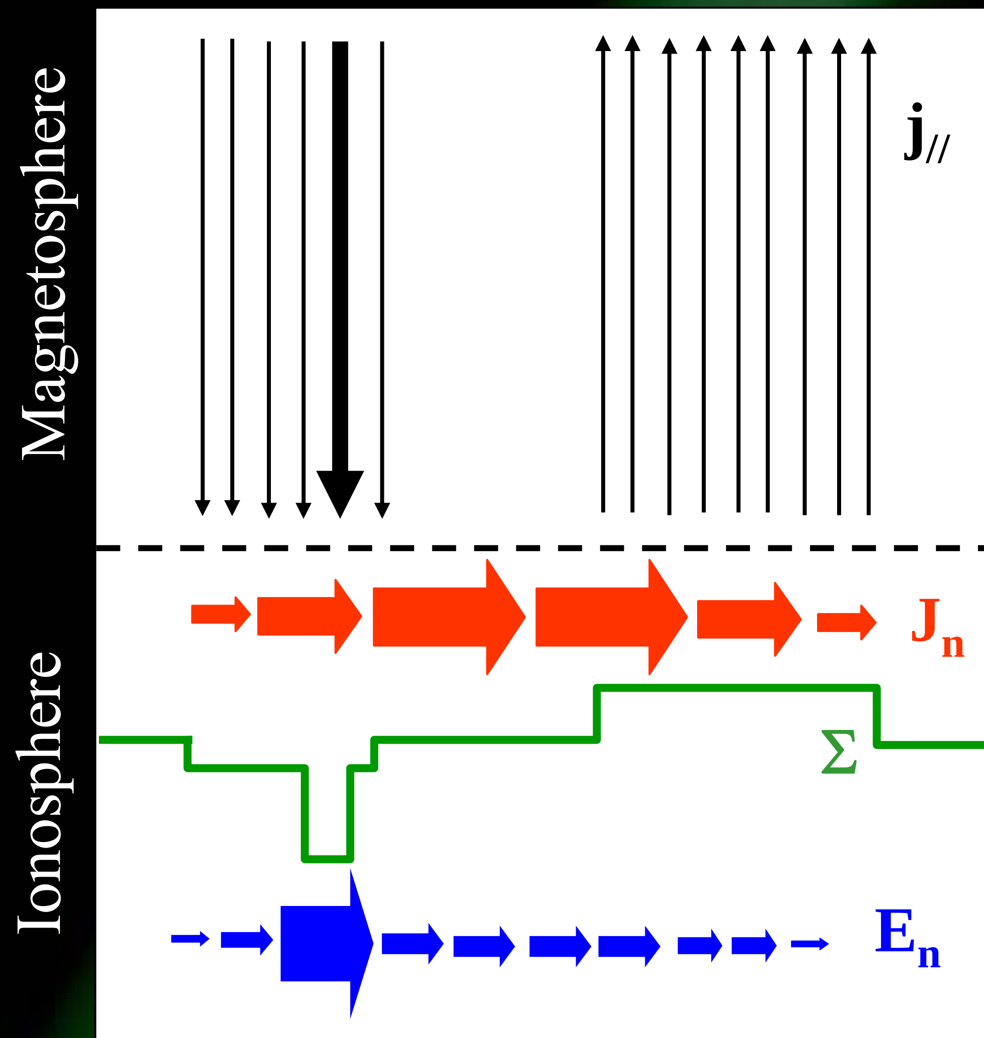


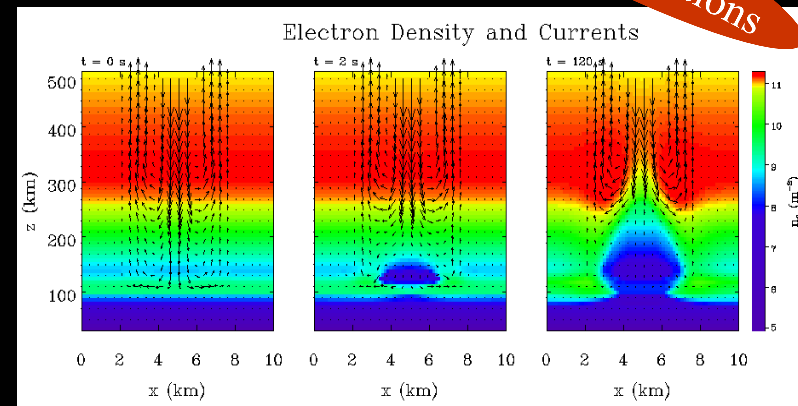


$$J_n = \int j_{\|} dn + \Sigma_{P,0} E_{n,0} + \Sigma_{H,0} E_t$$

$$\Sigma_P = \Sigma_{P,0} + \begin{cases} k_{down} j_{//} & \text{downward } j_{//} \\ 0 & \text{upward } j_{//} \end{cases}$$

$$\Sigma_P \geq \Sigma_{P,min}, \quad \Sigma_H = 2\Sigma_P$$

$$E_n = \frac{\Sigma_{P,0} E_{n,0}}{\Sigma_P} + \frac{\left(\Sigma_H - \Sigma_{H,0}\right) E_t}{\Sigma_P} + \frac{1}{\Sigma_P} \int j_{\|} dn$$

# *2004-02-18*
# *k* as a function of time

Fit $k = \kappa t \Rightarrow$

$\kappa = 1.9 \cdot 10^{-3}$ $Sm^2/\mu As$

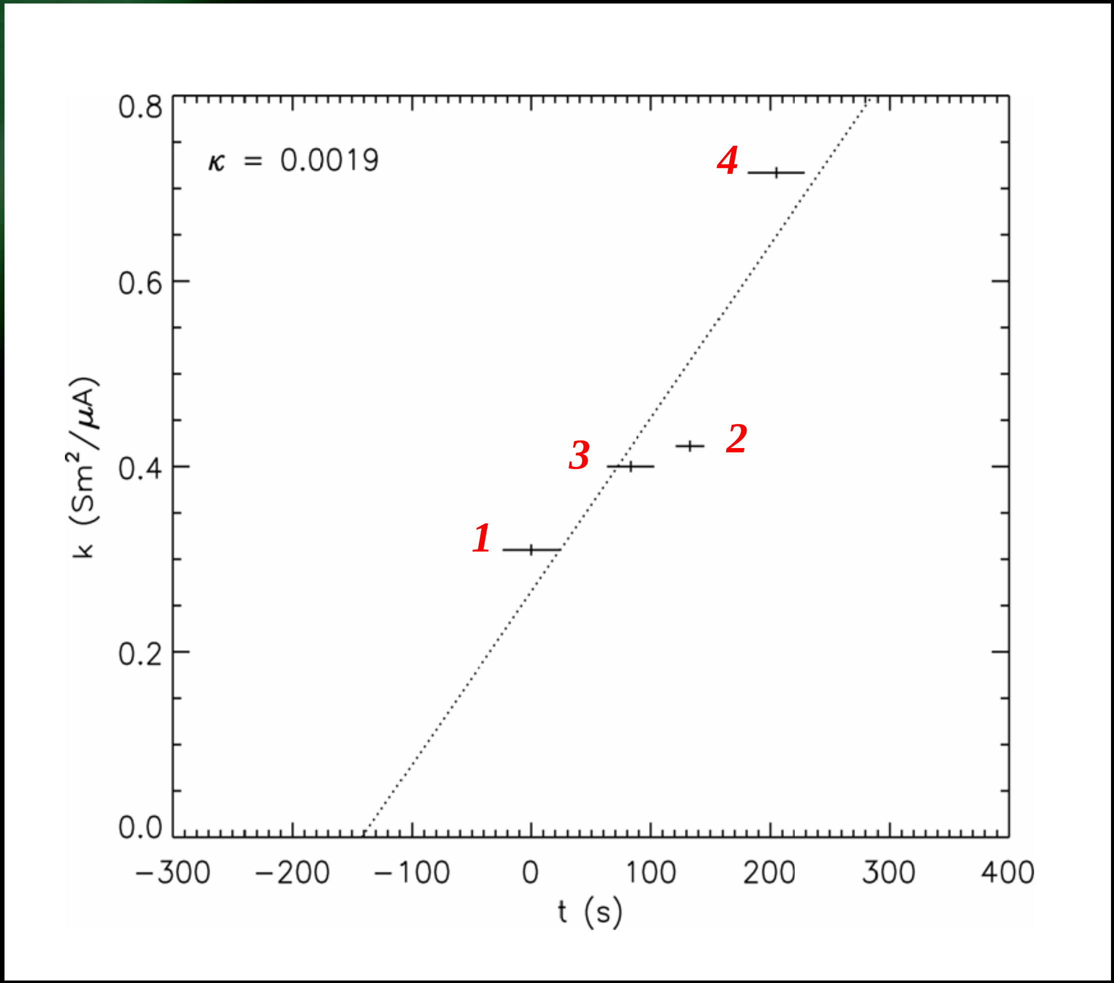


From simulations:

$1 \cdot 10^{-5} \leq \kappa \leq 2 \cdot 10^{-3}$ $Sm^2/\mu As$

Thank you for your attention!